AN OVERLAPPING DOMAIN DECOMPOSITION METHOD FOR THE REISSNER-MINDLIN PLATE WITH THE FALK-TU ELEMENTS

JONG HO LEE *

August 28, 2010

Abstract. The Reissner-Mindlin plate theory models a thin plate with thickness t. The condition numbers of finite element approximations of this model deteriorate badly as the thickness t of the plate converges to 0. In this paper, we develop an overlapping domain decomposition method for the Reissner-Mindlin plate model discretized by the Falk-Tu elements with the convergence rate which does not deteriorate when t converges to 0. It is shown that the condition number of this overlapping method is bounded by $C(1+\frac{H}{\delta})^3(1+log\frac{H}{h})^2$. Here H is the maximum diameter of the subdomains, δ the size of overlap between subdomains, and h the element size. Numerical examples are provided to confirm the theory.

Key words. domain decomposition, overlapping Schwarz, preconditioners, iterative methods, Reissner-Mindlin model, Falk-Tu elements, mixed finite element methods

AMS subject classifications. 65N55

1. Introduction. The Reissner-Mindlin plate theory is developed to describe the behavior of a thin plate. If we use standard low order polynomial elements to discretize a Reissner-Mindlin plate, we then can suffer from locking problems when the plate is thin and therefore the Kirchhoff condition, $\nabla w = \theta$, is too severe. For example, if we use continuous piecewise linear functions to approximate both the displacement and rotation variables with zero boundary condition, the rotation variables would be 0. To overcome that, many mixed elements have been developed, see [9, pp.195-232], [10, chapter 5.6], and [1, 2, 5–7, 16–19, 21, 22, 24, 26, 27, 30, 32].

The Kirchhoff (biharmonic) plate problem is related to the Reissner-Mindlin plate theory. For the Kirchhoff plate, see [10, chapter 6.5], [9] and [12, chapter 5.9]. These two models have similar interior solutions but differ significantly in a boundary layer of a width of order of t. It is known that as t converges to 0, the solution of the Reissner-Mindlin Plate model converges to the solution of the Kirchhoff Plate model; see [3] and [4].

There are many studies which develop preconditioners for the Kirchhoff plate problem, see [13–15, 25, 28]. [25] and [28] can be extended to the Reissner-Mindlin plate problem for elements which are spectrally equivalent to Kirchhoff plate elements. For MITC element approximation of the Reissner-Mindlin plate problem, a BDDC method has been developed, see [8].

The goal of this paper is to develop an overlapping domain decomposition method for the Reissner-Mindlin plate discretized by the Falk-Tu elements.

In section 2, we present the Reissner-Mindlin plate theory. In Section 3, we introduce the Falk-Tu elements. An overlapping domain decomposition method is introduced in section 4. We prove our bound in section 5 and provide some comments in sections 6 and 7. We report on some numerical results in section 8.

2. The Continuous Problem. Let the plate occupy the region $P_t = \Omega \times (-\frac{t}{2}, +\frac{t}{2})$, where Ω is a bounded domain of diameter 1 in $\mathbb{R}^2$. We are interested

*Courant Institute of Mathematical Science jlee@cims.nyu.edu, 251 Mercer Street, New York, NY 10012 This work has been supported by the National Science Foundation Grant DMS-0914954

in the case when the plate is thin, i.e., t is small. In this problem, we consider three displacement components u_i, i=1,2,3. We use a reduction of dimension for the z-direction, and assume the following four conditions, cf. [10, chapter 6.5]:

H1. The linearity hypothesis.

H2. The displacement in the z-direction does not depend on the z-coordinate.

H3. The points on the middle surface are deformed only in the z-direction.

H4. The normal stress σ_{33} vanishes.

Under the above hypotheses, we can write the displacement components as,

$$\begin{aligned} u_i(x,y,z) &= -z\theta_i(x,y), \quad \text{for i=1,2} \\ u_3(x,y,z) &= w(x,y). \end{aligned}$$

Here w is the *transversal displacement* and $\theta = (\theta_1, \theta_2)$ the *rotation*. If we adopt the Kirchhoff condition $\nabla w = \theta$, this becomes the Kirchhoff Plate model; see [10, chapter 6.5] and [9]. These two models have similar interior solutions but differ significantly in a boundary layer of a width of order of t. As t converges to 0, the solution of the Reissner-Mindlin Plate model converges to the solution of the Kirchhoff Plate model; see [3] and [4].

In the above setting, we solve the Reissner-Mindlin equations of the form

$$\begin{aligned} -\mathbf{div}\mathcal{C}\varepsilon(\theta) - \lambda t^{-2}(\nabla w - \theta) &= -\boldsymbol{f} \\ -\mathrm{div}(\nabla w - \theta) &= \lambda^{-1}t^2 g \end{aligned} \tag{2.1}$$

where $\mathcal{C} = \mathbf{A}^{-1}$, $\mathbf{A}\tau = (1+\nu)\tau/E - \nu tr(\tau)\mathbf{I}/E$, and $\mathbf{I}$ is the 2 by 2 identity matrix.

The related Reissner-Mindlin energy, see [10, chapter 6.6], is

$$J(\theta, w) = \frac{1}{2}\int_\Omega \mathcal{C}\varepsilon(\theta) : \varepsilon(\theta) + \frac{1}{2}\lambda t^{-2}\int_\Omega |\nabla w - \theta|^2 - \int_\Omega gw + \int_\Omega f\cdot\theta. \tag{2.2}$$

This problem can have a locking problem and we can handle that by using mixed finite element methods; see [10], [9]. By introducing the shear stress $\gamma = \lambda t^{-2}(\nabla w - \theta)$, we obtain the following variational problem, cf. [10, chapter 6.6], [9], [8]:

Find $\theta \in \boldsymbol{H}_0^1(\Omega), w \in H_0^1(\Omega), \gamma \in \boldsymbol{L}^2(\Omega)$ such that

$$\begin{aligned} a(\theta,\phi) + (\gamma, \nabla v - \phi) &= (g,v) - (\boldsymbol{f},\phi), \quad && \phi \in \boldsymbol{H}_0^1(\Omega), v \in H_0^1(\Omega) \\ (\nabla w - \theta, \eta) - \lambda^{-1}t^2(\gamma,\eta) &= 0, && \eta \in \boldsymbol{L}^2(\Omega). \end{aligned} \tag{2.3}$$

3. Discretization by the Falk-Tu Element. We use the following conforming elements, i.e., $\Theta_h \subset \boldsymbol{H}_0^1(\Omega)$, $W_h \subset H_0^1(\Omega)$, and $\Gamma_h \subset \boldsymbol{L}^2(\Omega)$. Let Π be the $\boldsymbol{L}^2$ projector of $\boldsymbol{H}_0^1(\Omega)$ onto Γ_h. Then, as in [10], [9], the discrete problem becomes:

Find $\theta_h \in \Theta_h, w_h \in W_h, \gamma_h \in \Gamma_h$ such that

$$\begin{aligned} a(\theta_h,\phi) + (\gamma_h, \nabla v - \Pi\phi) &= (g,v) - (\boldsymbol{f},\phi), \quad && \phi \in \Theta_h, v \in W_h \\ (\nabla w_h - \Pi\theta_h, \eta) - \lambda^{-1}t^2(\gamma_h,\eta) &= 0, && \eta \in \Gamma_h. \end{aligned} \tag{3.1}$$

In the Falk-Tu element method, see [9], [23], we choose

$$\Theta_h = \boldsymbol{M}_{1,0}^1 + \boldsymbol{B}^4,\ W_h = M_{1,0}^2,\ \Gamma_h = \boldsymbol{M}_0^1$$

on the triangulation. Here $\boldsymbol{M}_{a,0}^k$ is the space of piecewise kth order polynomials in $\boldsymbol{H}_0^a(\Omega)$, $M_{a,0}^k$ the space of piecewise kth order polynomials in $H_0^a(\Omega)$, $\boldsymbol{M}_a^k$ the space of piecewise kth order polynomials in $\boldsymbol{H}^a$, and $\boldsymbol{B}^k$ the space of piecewise kth order polynomial bubble functions.

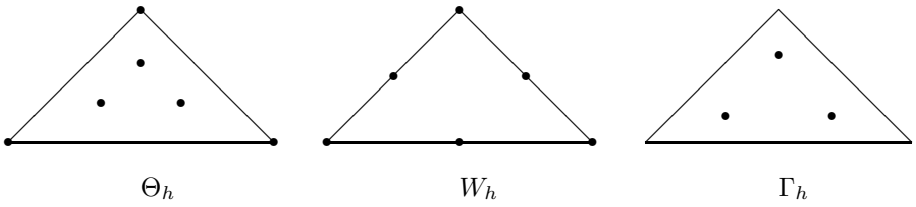

FIG. 3.1. *the Falk-Tu element with k=2.*

Because we choose a discontinuous stress variable, we can eliminate it on the element level as in [20], [8]. Then, the problem becomes :

Find $\theta_h \in \Theta_h, w_h \in W_h$ such that

$$a(\theta_h, \phi) + \frac{\lambda}{t^2}(\nabla w_h - \Pi\theta_h, \nabla v - \Pi\phi) = (g, v) - (\boldsymbol{f}, \phi), \quad \phi \in \Theta_h, v \in W_h. \quad (3.2)$$

The discrete Reissner-Mindlin energy

$$a(\theta_h, \theta_h) + \frac{\lambda}{t^2}(\nabla w_h - \Pi\theta_h, \nabla w_h - \Pi\theta_h) \quad (3.3)$$

will be estimated later in the proof.

For natural boundary conditions, the dimension of the null space of this Reissner-Mindlin energy is 3. The first null element is given by $w = 1$ and $\theta = (0, 0)$, the second by $w = x$ and $\theta = (1, 0)$, and the third by $w = y$ and $\theta = (0, 1)$. These null space functions will play an important role for the subdomain problems defined later.

We have the following error estimate. For a proof, we refer to the lecture notes edited by Boffi and Gastaldi [9, pp.213-216].

THEOREM 3.1. *For sufficiently smooth solutions of the continuous problem, we have*

$$\|\theta - \theta_h\|_0 + \|w - w_h\|_1 \leq Ch^2(\|\mathbf{f}\|_0 + \|g\|_0) \quad (3.4)$$

where C is independent of h.

4. The Domain Decomposition Methods.

4.1. Decomposition of the Domain. We decompose the given domain Ω into a set of shape regular nonoverlapping subdomains $\{\Omega_i\}_{i=1}^N$, see [33], [10], [12]. We assume, when developing the theory, that the subdomains are triangles in the plane. H is the maximum of the diameters of the subdomains. We then, decompose each subdomain into quasi-uniform and shape-regular elements and introduce our finite element spaces on this triangulation. The nodes of the fine elements should match across the interface. We extend each subdomain by adding layers of elements and denote the set of N extended subdomains by $\{\Omega_i'\}_{i=1}^N$. We denote the size of the overlap between extended subdomains by δ_i and assume $\frac{H_i}{\delta_i}$, i=1,...,N, is bounded from below. For more details, see [33, chapters 2 and 3].

4.2. Abstract Schwarz Methods. We consider a finite dimensional space V on the triangulation. Discretizing equation (3.2) by the finite element method, we will get a linear system

$$Au = f \quad (4.1)$$

with A symmetric, positive definite and very ill conditioned for small t.

We will consider a family of spaces $\{V_i$, i=0,...,N$\}$ and construct *extension* operators

$$R_i^T : V_i \to V;$$

The subspace V_0 will usually be associated with a coarse problem and the remaining spaces are defined on the extended subdomains Ω_i'. The V_i, i=1,...,N, are contained in $(H_0^1(\Omega_i'))^3$. We obtain a Schwarz decomposition

$$V = R_0^T V_0 + \sum_{i=1}^{N} R_i^T V_i.$$

We introduce exact local problems on the local spaces V_i such that with $A_i = R_i A R_i^T$, the Schwarz operators $P_i : V \to V$ are defined by $R_i^T A_i^{-1} R_i A$ for $i = 0, ..., N$. With exact solvers, the P_is are projections. We define the additive Schwarz preconditioner by

$$A_{ad}^{-1} := \sum_{i=0}^{N} R_i^T A_i^{-1} R_i$$

and the additive Schwarz operator by

$$P_{ad} := \sum_{i=0}^{N} P_i.$$

We know that a stable decomposition of the space V into V_i implies that the additive operator has a condition number bounded by $(N^c + 1)C_0^2$ where C_0 is a parameter related to the stable decomposition and N^c is a constant related to the coloring of the decomposition $\{\Omega_i'\}$. For more detail, see [33, chapters 2 and 3]. In numerical examples reported later, we will use uniform triangles as subdomains and N^c will not be larger than 13. Therefore, what remains is to find a stable decomposition of V into V_i. We are then able to use the abstract theory of Schwarz methods.

4.3. The Discrete Harmonic Extension. On each nonoverlapping subdomain Ω_i, we define an *extension* operator

$$\tilde{R}_i^T : \tilde{V}_i \to V$$

where $\tilde{V}_i$ is a subspace defined on Ω_i with natural boundary conditions. $\tilde{R}_i^T$ is similar to R_i^T but it is defined on Ω_i only. We then obtain the linear system

$$\tilde{A}_i u_i = f_i \text{ with } u_i \in \tilde{V}_i$$

where $\tilde{A}_i = \tilde{R}_i A \tilde{R_i^T}$.

We can rewrite $\tilde{A}_i$ with respect to the components of the interface and interior basis functions of $\tilde{A}_i$.

$$\begin{bmatrix} \tilde{A}_{i,II} & \tilde{A}_{i,I\Gamma} \\ \tilde{A}_{i,\Gamma I} & \tilde{A}_{i,\Gamma\Gamma} \end{bmatrix} \begin{bmatrix} u_{i,I} \\ u_{i,\Gamma} \end{bmatrix} = \begin{bmatrix} f_{i,I} \\ f_{i,\Gamma} \end{bmatrix}.$$

Given $u_{i,\Gamma}$, we can calculate the interior values by solving

$$\tilde{A}_{i,II} u_{i,I} + \tilde{A}_{i,I\Gamma} u_{i,\Gamma} = 0. \tag{4.2}$$

This is a discrete harmonic function on Ω_i, see [33, chapter 4]. When we define the coarse basis functions, we will define their values on the interface only and then calculate discrete harmonic extensions to the interior values of subdomains. We define each coarse basis function in detail in section 5. For the coarse problem, we will also use an exact solver.

5. The Algorithm and the Results.

5.1. Definition of the Operator $\mathcal{C}$ and Bilinear Forms. We will consider the operator $\mathbf{A}$ in more detail and find the relation between $a(\theta,\theta)$ and H^1 norm of θ. Let,

$$\begin{aligned}\mathbf{A}\tau &:= \frac{1+\nu}{E}\tau - \frac{\nu tr(\tau)}{E}I \\ &= \frac{1}{E}\begin{pmatrix} 1 & -\nu & 0 \\ -\nu & 1 & 0 \\ 0 & 0 & 1+\nu \end{pmatrix}\begin{pmatrix} \tau_{11} \\ \tau_{22} \\ \tau_{12} \end{pmatrix}.\end{aligned} \tag{5.1}$$

Then $\mathcal{C}$, the inverse of $\mathbf{A}$, is defined by

$$\begin{aligned}\mathcal{C}\varepsilon &:= \mathbf{A}^{-1}\varepsilon \\ &= \frac{E}{(1-\nu^2)}\begin{pmatrix} 1 & \nu & 0 \\ \nu & 1 & 0 \\ 0 & 0 & 1-\nu \end{pmatrix}\begin{pmatrix} \varepsilon_{11} \\ \varepsilon_{22} \\ \varepsilon_{12} \end{pmatrix} \\ &= \frac{E}{2(1+\nu)}\begin{pmatrix} \frac{2}{1-\nu} & \frac{2\nu}{1-\nu} & 0 \\ \frac{2\nu}{1-\nu} & \frac{2}{1-\nu} & 0 \\ 0 & 0 & 2 \end{pmatrix}\begin{pmatrix} \varepsilon_{11} \\ \varepsilon_{22} \\ \varepsilon_{12} \end{pmatrix} \\ &= \mu\begin{pmatrix} \frac{2}{1-\nu} & \frac{2\nu}{1-\nu} & 0 \\ \frac{2\nu}{1-\nu} & \frac{2}{1-\nu} & 0 \\ 0 & 0 & 2 \end{pmatrix}\begin{pmatrix} \varepsilon_{11} \\ \varepsilon_{22} \\ \varepsilon_{12} \end{pmatrix}\end{aligned} \tag{5.2}$$

where

$$\mu := \frac{E}{2(1+\nu)}. \tag{5.3}$$

With

$$\varepsilon(\theta) := \frac{1}{2}\begin{pmatrix} 2\theta_x^1 & \theta_x^2+\theta_y^1 \\ \theta_x^2+\theta_y^1 & 2\theta_y^2 \end{pmatrix}, \tag{5.4}$$

define

$$\begin{aligned}a(\theta,\phi) &:= \int_\Omega (\mathcal{C}\varepsilon(\theta),\varepsilon(\phi)) \\ &= \int_\Omega \left(\begin{pmatrix} \frac{2\mu}{1-\nu}\theta_x^1 + \frac{2\mu\nu}{1-\nu}\theta_y^2 \\ \frac{2\mu}{1-\nu}\theta_y^2 + \frac{2\mu\nu}{1-\nu}\theta_x^1 \\ \mu(\theta_x^2+\theta_y^1) \end{pmatrix}, \begin{pmatrix} \phi_x^1 \\ \phi_y^2 \\ \frac{1}{2}(\phi_x^2+\phi_y^1) \end{pmatrix}\right) \\ &= \int_\Omega (\frac{2\mu}{1-\nu}\theta_x^1\phi_x^1 + \frac{2\mu\nu}{1-\nu}\theta_y^2\phi_x^1 + \frac{2\mu}{1-\nu}\theta_y^2\phi_y^2) + \\ &\quad \int_\Omega (\frac{2\mu\nu}{1-\nu}\theta_x^1\phi_y^2 + (\phi_x^2+\phi_y^1)(\theta_x^2+\theta_y^1)\mu).\end{aligned} \tag{5.5}$$

Thus,

$$\begin{aligned}\frac{a(\theta,\phi)}{\mu} &= \int_\Omega 2(\theta_x^1\phi_x^1+\theta_y^2\phi_y^2+\frac{1}{2}(\theta_x^2+\theta_y^1)(\phi_x^2+\phi_y^1))+\\ &\quad \int_\Omega \frac{2\nu}{1-\nu}(\theta_x^1\phi_x^1+\theta_y^2\phi_y^2+\theta_y^2\phi_x^1+\theta_x^1\phi_y^2)\\ &= 2\int_\Omega \varepsilon(\theta):\varepsilon(\phi)+\frac{2\nu}{1-\nu}\int_\Omega \mathrm{div}\theta\mathrm{div}\phi,\end{aligned}$$

or

$$\begin{aligned}a(\theta,\phi) &= 2\int_\Omega \mu\varepsilon(\theta):\varepsilon(\phi)+\frac{2\mu\nu}{1-\nu}\int_\Omega \mathrm{div}\theta\mathrm{div}\phi\\ &= \int_\Omega 2\mu\varepsilon(\theta):\varepsilon(\phi)+\lambda\int_\Omega \mathrm{div}\theta\mathrm{div}\phi \qquad (5.6)\\ &\quad \text{where } \lambda := \frac{2\mu\nu}{1-\nu}.\end{aligned}$$

The bilinear form $a(\theta,\theta)$ is that of the standard linear elasticity operator. We can easily show that $a(\theta,\theta)$ is bounded by the square of the H^1-seminorm of θ if the Lamé parameters μ and λ are bounded. More precisely, we get the bound

$$a(\theta,\theta)\le \max(2\mu,\lambda)|\theta|^2_{H^1}. \qquad (5.7)$$

From now on, let $\tilde{m} := \max(2\mu,\lambda)$.
We will use the scaled H^1 norm for each subdomain:

$$||u||^2_{H^1(\Omega_i)} = |u|^2_{H^1(\Omega_i)}+\frac{1}{H_i^2}||u||^2_{L^2(\Omega_i)}. \qquad (5.8)$$

5.2. Discrete Harmonic Extension. The energy of the interior part of u, which is orthogonal to discrete harmonic functions in a-seminorm, can be bounded by the sum of the energy of each local component of u. Therefore, it is enough to consider discrete harmonic functions when establishing the stable decomposition. From now on, we will assume that u is discrete harmonic in each subdomain.

Because the support of each bubble function is contained in a single element, the bubble functions are determined by the values of the piecewise linear parts of θ and w if u is discrete harmonic to minimize the Reissner-Mindlin energy. Therefore, we can consider the bubble function as a dependent functions in the harmonic extension function.

Let us consider one element K only and assume that the piecewise linear part of θ and w are already determined. Let θ_L be the piecewise linear part of θ. Using the bubble basis functions θ_B^k, k=1,2,...6, we can write $\nabla w-\Pi\theta_L=\sum_{k=1}^6\beta_k\theta_B^k$ with certain coefficients β_k.

Note that the square of the L^2-norm of the divergence of θ_B is positive definite. Therefore, the two components of the a-seminorm are equivalent over the bubble function space and $\mathrm{a}(\theta_B,\theta_B)$ is equivalent to $\tilde{m}|\theta_B|^2_{H^1}$.

Let us write the bubble function on the element K as $\theta_B=\sum_{k=1}^6\alpha_k\beta_k\theta_B^k$. We can then choose optimal coefficients $\alpha_k,\ k=1,...,6$ for the bubble functions to minimize the Reissner-Mindlin energy of u. We know that the a-seminorm does not depend on the scaling and the square of the L^2-norm of bubble functions is on the order of h^2.

Let β be diagonal matrix with the diagonal entries $\beta_1,\ \beta_2, ..., \beta_6$, and let $\alpha = (\alpha_1, \alpha_2, ..., \alpha_6)^t$. Let F and G be the matrices for the a-seminorm and the L^2-norm of the bubble functions on a reference element, respectively. Let $\tilde{F} = \beta^t F \beta$, $\tilde{G} = \beta^t G \beta$, and let $\mathbf{1}$ be the 6-dimensional column vector with all entries 1. We know that $h^2 \mathbf{1}^t \beta^t \beta \mathbf{1}$ is equivalent to $||\nabla w - \theta_L||^2_{L^2(K)}$. Then Reissner-Mindlin energy of $(\theta_L + \alpha\beta\theta_B^k, w)$ is equivalent to

$$a(\theta_L, \theta_L) + \tilde{m}\alpha^t \tilde{F}\alpha + \frac{h^2}{t^2}(\mathbf{1}-\alpha)^t \tilde{G}(\mathbf{1}-\alpha).$$

This is minimized by

$$\begin{aligned} \alpha &= \frac{h^2}{t^2}\tilde{K}^{-1}\tilde{G}\mathbf{1} \qquad \text{where} \\ K &:= \tilde{m}F + \frac{h^2}{t^2}G \quad \text{and} \\ \tilde{K} &:= \beta^t K \beta \\ &= \tilde{m}\tilde{F} + \frac{h^2}{t^2}\tilde{G} \end{aligned}$$

and

$$\mathbf{1} - \alpha = \tilde{m}\tilde{K}^{-1}\tilde{F}\mathbf{1}.$$

If we plug this α into the above energy formula, the Reissner-Mindlin energy is equivalent to

$$\begin{aligned} &a(\theta_L, \theta_L) + \tilde{m}\frac{h^2}{t^2}\frac{h^2}{t^2}\mathbf{1}^t\tilde{G}\tilde{K}^{-1}\tilde{F}\tilde{K}^{-1}\tilde{G}\mathbf{1} + \tilde{m}^2\frac{h^2}{t^2}\mathbf{1}^t\tilde{F}\tilde{K}^{-1}\tilde{G}\tilde{K}^{-1}\tilde{F}\mathbf{1} \\ &= a(\theta_L, \theta_L) + \tilde{m}\frac{h^2}{t^2}\mathbf{1}^t\beta^t(\frac{h^2}{t^2}GK^{-1}FK^{-1}G + \tilde{m}FK^{-1}GK^{-1}F)\beta\mathbf{1}. \end{aligned}$$

Because F, G and K are positive definite, so are $GK^{-1}FK^{-1}G$ and $FK^{-1}GK^{-1}F$. We can bound the quadratic forms of these two positive definite matrices by each other in terms of $\tilde{m}$, h and t. We then find that $GK^{-1}FK^{-1}G$ is equivalent to $c^{-2}\mathbf{I}$ where $c := \tilde{m} + \frac{h^2}{t^2}$. Similarly, $FK^{-1}GK^{-1}F$ is equivalent to $c^{-2}\mathbf{I}$.

The Reissner-Mindlin energy is equivalent to

$$\begin{aligned} &a(\theta_L, \theta_L) + \tilde{m}\frac{h^2}{t^2}\mathbf{1}^t\beta^t(\frac{h^2}{t^2}c^{-2}\mathbf{I} + \tilde{m}c^{-2}\mathbf{I})\beta\mathbf{1} \\ &= a(\theta_L, \theta_L) + \tilde{m}\frac{h^2}{t^2}\mathbf{1}^t\beta^t(c^{-1}\mathbf{I})\beta\mathbf{1} \\ &= a(\theta_L, \theta_L) + c^{-1}\tilde{m}\frac{h^2}{t^2}\mathbf{1}^t\beta^t\beta\mathbf{1} \\ &= a(\theta_L, \theta_L) + \frac{\tilde{m}}{\tilde{m}t^2 + h^2}h^2\mathbf{1}^t\beta^t\beta\mathbf{1}. \end{aligned}$$

Using the equivalence of $h^2\mathbf{1}^t\beta^t\beta\mathbf{1}$ and $||\nabla w - \theta_L||^2_{L^2(K)}$, the Reissner-Mindlin energy is equivalent to

$$a(\theta_L, \theta_L) + \frac{\tilde{m}||\nabla w - \theta_L||^2_{L^2(K)}}{\tilde{m}t^2 + h^2}. \tag{5.9}$$

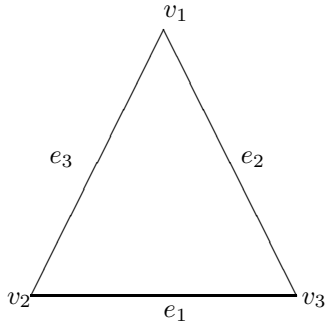

FIG. 5.1. *One subdomain and its vertices and edges.*

Overall, we can conclude that minimizing the Reissner-Mindlin energy over the $(\theta_L,\ \theta_B,\ w)$ space is equivalent to minimizing the expression of the equation (5.9) over the $(\theta_L,\ w)$ space. This is called the stabilized Reissner-Mindlin energy of the $(\theta_L,\ w)$ space.

There are two terms: $a(\theta_L, \theta_L)$ and $\frac{\tilde{m}}{\tilde{m}t^2+h^2}||\nabla w - \theta_L||^2_{L^2}$ in the stabilized Reissner-Mindlin energy. The a-seminorm increases linearly with $\tilde{m}$ and the ratio between the two terms is $\frac{1}{\tilde{m}t^2+h^2}$. If t=0, this ratio is $\frac{1}{h^2}$ and larger than 1. If this ratio is small, then the problem is close to the linear elasticity problem; this ratio should be large for Reissner-Mindlin plate problem to be physically reasonable. If t is sufficiently small, then we can find $\tilde{h}$ such that $\tilde{m}t^2 + h^2 = \tilde{h}^2$ and we can consider the case of t$>$ 0 as being similar to the case of t$=$ 0 with a mesh size $\tilde{h}$.

Therefore, if t is bounded from above, we can consider t as being 0. In interesting problems for a Reissner-Mindlin plate, t is in this good range and we, therefore assume that t is 0 from now on.

5.3. The Case of t=0.

5.3.1. The Coarse Problem. We now provide details on the coarse basis functions. We define them on the interface and use their discrete harmonic extensions. We consider the subdomains Ω_i, one by one, to define the coarse basis functions. From now on, we consider only one of the floating subdomains Ω_i with $\partial\Omega_i \bigcap \partial\Omega = \emptyset$.

For each θ_i, i=1,2, we define a vertex basis function which vanishes at all interface nodes except at a subdomain vertex where its value is 1. We denote these vertex basis functions by θ^0_{i,v_k}, i=1,2, k=1,2,3. Because there are two components of θ, we have 6 vertex basis functions for each subdomain.

LEMMA 5.1. *The Reissner-Mindlin energy of the vertex basis function θ^0_{i,v_k} is bounded by $C\tilde{m}$ where C does not depend on H, h and δ, but depends on the shape regularity of the elements.*

Proof. We can find a bubble function θ_B such that the $\Pi\theta_B + \theta_L = 0$ where θ_L is a piecewise continuous linear functions with zero values at the interface and interior nodes except at the subdomain vertex being considered. This θ_B vanishes except in the elements which contain the subdomain vertex. The number of such elements are bounded by the shape regularity. The H^1-seminorm of this function is bounded by a constant. Because $\nabla w = \Pi\theta$, the Reissner-Mindlin energy is equal to the square of the a-seminorm and we can bound the Reissner-Mindlin energy in terms of the square of the H^1-seminorm. □

For the other coarse basis functions, we need to prove several lemmas.

LEMMA 5.2. *Let $\xi_1,\ \xi_2,\ \xi_3$ be the values of the barycentric functions of the subdo-*

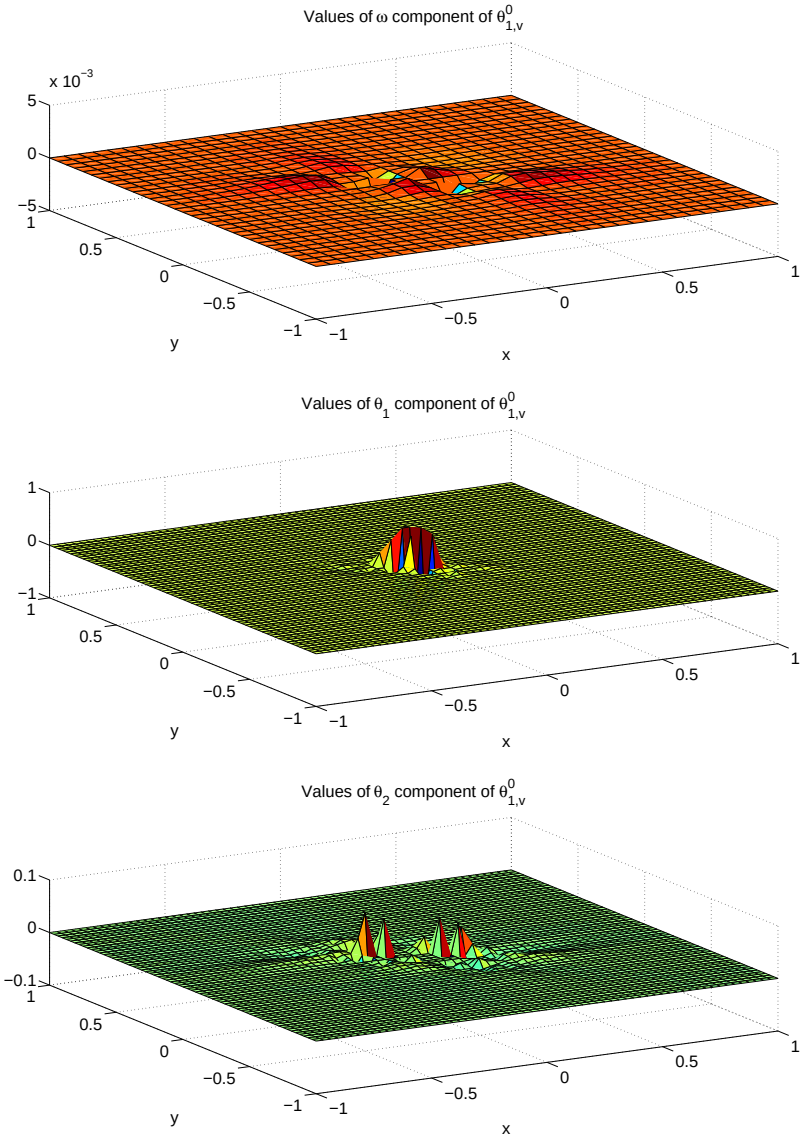

FIG. 5.2. *3d plot of the θ vertex basis function $\theta^0_{1,v}$.*

main at (x,y). Let

$$\Upsilon_i := \frac{\frac{1}{\xi_i^2}}{\frac{1}{\xi_1^2} + \frac{1}{\xi_2^2} + \frac{1}{\xi_3^2}}. \tag{5.10}$$

Then, the gradient of Υ_i is bounded by $\frac{C}{r}$ where r is the minimum distance to the two

vertices of the edge i. The second order partial derivatives of Υ_i *are bounded by* $\frac{C}{r^2}$.

Proof. Without loss of generality, we prove the lemma for Υ_1 only. We use the Figure 5.1 of the triangle to define the indices of e_1, e_2, e_3, v_1, v_2, and v_3. Let $f := \xi_2^2\xi_3^2$ and $g := \xi_1^2\xi_2^2 + \xi_1^2\xi_3^2$. Then,

$$\begin{aligned}\Upsilon_1 &= \frac{\frac{1}{\xi_1^2}}{\frac{1}{\xi_1^2}+\frac{1}{\xi_2^2}+\frac{1}{\xi_3^2}} \\ &= \frac{\xi_2^2\xi_3^2}{\xi_2^2\xi_3^2+\xi_1^2\xi_2^2+\xi_1^2\xi_3^2} \\ &= \frac{f}{f+g}.\end{aligned}$$

We can easily show that $f + g \geq Cmin(\tilde{r}^2, r^2)$ where $\tilde{r}$ is the minimum distance to the other vertex v_1 of the triangle which is not on the edge e_1. $min(\tilde{r}, r)$ is the minimum distance to the three vertices of the triangle.

For f, we can also show that $f \leq Cr^2\tilde{r}^4$.

We calculate the first order partial derivatives of f,

$$\begin{aligned}f_x &= 2\xi_2\xi_{2,x}\xi_3^2 + 2\xi_3\xi_{3,x}\xi_2^2 \\ f_y &= 2\xi_2\xi_{2,y}\xi_3^2 + 2\xi_3\xi_{3,y}\xi_2^2,\end{aligned}$$

and find that $|f_x| \leq Cr\tilde{r}^3$ and $|f_y| \leq Cr\tilde{r}^3$.

The second order partial derivatives of f are

$$\begin{aligned}f_{xx} &= 2((\xi_{2,x})^2\xi_3^2 + \xi_{2,xx}\xi_2\xi_3^2 + 2\xi_{3,x}\xi_{2,x}\xi_3\xi_2 \\ &\quad +(\xi_{3,x})^2\xi_2^2 + \xi_{3,xx}\xi_3\xi_2^2 + 2\xi_{2,x}\xi_{3,x}\xi_3\xi_2) \\ f_{xy} &= 2(\xi_{2,y}\xi_{2,x}\xi_3^2 + \xi_2\xi_{2,xy}\xi_3^2 + 2\xi_{2,x}\xi_{3,y}\xi_2\xi_3 \\ &\quad +\xi_{3,y}\xi_{3,x}\xi_2^2 + \xi_{3,xy}\xi_3\xi_2^2 + 2\xi_{3,x}\xi_{2,y}\xi_3\xi_2) \\ f_{yy} &= 2((\xi_{2,y})^2\xi_3^2 + \xi_{2,yy}\xi_2\xi_3^2 + 2\xi_{3,y}\xi_{2,y}\xi_3\xi_2 \\ &\quad +(\xi_{3,y})^2\xi_2^2 + \xi_{3,yy}\xi_3\xi_2^2 + 2\xi_{2,y}\xi_{3,y}\xi_3\xi_2),\end{aligned}$$

and we find that $|f_{xx}|^2 \leq C\tilde{r}^2$, $|f_{xy}|^2 \leq C\tilde{r}^2$, and $|f_{yy}|^2 \leq C\tilde{r}^2$. Similarly, we can calculate the first and second order partial derivatives of g and obtain a bound of them by taking the maximum of the bounds of the two terms in g. We find that $|g| \leq Cr^2\tilde{r}^2$, $|g_x| \leq Cr\tilde{r}$, $|g_y| \leq Cr\tilde{r}$, $|g_{xx}|^2 \leq C$, $|g_{xy}|^2 \leq C$, and $|g_{yy}|^2 \leq C$.

We next calculate the partial derivative of Υ_1 with respect to x and find

$$\begin{aligned}\frac{\partial\Upsilon_1}{\partial x} &= \frac{f_x(f+g) - f(f_x+g_x)}{(f+g)^2} \\ &= \frac{gf_x - fg_x}{(f+g)^2}.\end{aligned}$$

If we use the bounds just derived, then

$$\begin{aligned}|\frac{\partial \Upsilon_1}{\partial x}| &\leq \frac{Cr^2\tilde{r}^2 r\tilde{r}^3 + Cr^2\tilde{r}^4 r\tilde{r}}{Cmin(r^2,\tilde{r}^2)^2} \\ &\leq Cr^3\tilde{r}^5 max(r^{-4},\tilde{r}^{-4}) \\ &\leq Cmax(r^{-1}\tilde{r}^5, r^3\tilde{r}) \\ &\leq Cmax(r^{-1},1) \\ &\leq \frac{C}{r}.\end{aligned}$$

Similarly, we get $|\frac{\partial \Upsilon_1}{\partial y}| \leq \frac{C}{r}$.

For the second order derivative of Υ_1, we have

$$\begin{aligned}\frac{\partial^2 \Upsilon_1}{\partial x^2} &= \frac{(gf_{xx} + g_x f_x - f_x g_x - f g_{xx})(f+g)^2}{(f+g)^4} - \frac{2(f+g)(f_x+g_x)(gf_x - fg_x)}{(f+g)^4} \\ &= \frac{(gf_{xx} - fg_{xx})(f+g) - 2(f_x+g_x)(gf_x - fg_x)}{(f+g)^3}.\end{aligned}$$

This can be bounded by

$$\begin{aligned}\left|\frac{\partial^2 \Upsilon_1}{\partial x^2}\right| &\leq C\frac{(r^2\tilde{r}^2\tilde{r}^2 + r^2\tilde{r}^4)(r^2\tilde{r}^4 + r^2\tilde{r}^2) + (r\tilde{r}^3 + r\tilde{r})(r^2\tilde{r}^2 r\tilde{r}^3 + r^2\tilde{r}^4 r\tilde{r})}{(f+g)^3} \\ &\leq C\frac{(r^2\tilde{r}^4)(r^2\tilde{r}^2) + (r\tilde{r})(r^3\tilde{r}^5)}{(f+g)^3} \\ &\leq C\frac{r^4\tilde{r}^6 + r^4\tilde{r}^6}{min(r^6,\tilde{r}^6)} \\ &\leq Cr^4\tilde{r}^6 max(r^{-6},\tilde{r}^{-6}) \\ &\leq Cmax(r^{-2}\tilde{r}^6, r^4) \\ &\leq Cmax(r^{-2},1) \\ &\leq \frac{C}{r^2}.\end{aligned}$$

Similarly, we get $|\frac{\partial^2 \Upsilon_1}{\partial y^2}| \leq \frac{C}{r^2}$.

Also,

$$\begin{aligned}\frac{\partial^2 \Upsilon_1}{\partial x \partial y} &= \frac{(g_y f_x + g f_{xy} - f_y g_x - f g_{xy})(f+g)^2}{(f+g)^4} - \frac{2(f+g)(f_y+g_y)(gf_x - fg_x)}{(f+g)^4} \\ &= \frac{(g_y f_x + g f_{xy} - f_y g_x - f g_{xy})(f+g)}{(f+g)^4} - \frac{2(f_y+g_y)(gf_x - fg_x)}{(f+g)^3}.\end{aligned}$$

This can be bounded by

$$\begin{aligned}\left|\frac{\partial^2 \Upsilon_1}{\partial x \partial y}\right| &\leq C\frac{(r^2\tilde{r}^4)(r^2\tilde{r}^2) + (r\tilde{r})(r^3\tilde{r}^5)}{(f+g)^3} \\ &\leq Cr^4\tilde{r}^6 max(r^{-6},\tilde{r}^{-6}) \\ &\leq Cmax(r^{-2}\tilde{r}^6, r^4) \\ &\leq \frac{C}{r^2}.\end{aligned}$$

□

LEMMA 5.3. *Under the same assumptions as in Lemma 5.2, the gradient of Υ_i in (5.10) vanishes on the edges of a triangle.*

Proof. In the proof of Lemma 5.2, we have established that

$$\frac{\partial \Upsilon_1}{\partial x} = \frac{g f_x - f g_x}{(f+g)^2}$$

We have

$$\begin{aligned} g f_x &= (\xi_1^2\xi_2^2 + \xi_1^2\xi_3^2)(2\xi_2\xi_{2,x}\xi_3^2 + 2\xi_3\xi_{3,x}\xi_2^2) \\ &= 2\xi_1^2\xi_2\xi_3(\xi_2^2 + \xi_3^2)(\xi_{2,x}\xi_3 + \xi_{3,x}\xi_2). \end{aligned}$$

Therefore, this term vanishes on the edges of a triangle. Similarly,

$$\begin{aligned} f g_x &= \xi_2^2\xi_3^2(2\xi_1\xi_{1,x}\xi_2^2 + 2\xi_2\xi_{2,x}\xi_1^2 + 2\xi_1\xi_{1,x}\xi_3^2 + 2\xi_3\xi_{3,x}\xi_1^2) \\ &= \xi_1\xi_2^2\xi_3^2(2\xi_{1,x}\xi_2^2 + 2\xi_2\xi_{2,x}\xi_1 + 2\xi_{1,x}\xi_3^2 + 2\xi_3\xi_{3,x}\xi_1) \end{aligned}$$

which also vanishes on the edges. □

LEMMA 5.4. *We define Υ_i by equation (5.10) as in Lemma 5.2. Let M be a C^2 function on the closure of the triangle. For a given edge e_i, we assume that M goes to 0 at least linearly at the two vertices of the edge e_i. Then, the gradient of $M\Upsilon_i$ is bounded by a constant and the second order partial derivatives of $M\Upsilon_i$ are bounded by $\frac{C}{r}$, where r is the minimum distance to the two vertices of the edge i. The value of $M\Upsilon_i$ is equal to that of M on the edge e_i and to 0 on the other edges. The gradient of $M\Upsilon_i$ is equal to that of M on the edge e_i and to 0 on the other edges.*

Proof. Let us consider the edge e_1. Let $\tilde{M} = M\Upsilon_1$.

It is easy to see that the value of $\tilde{M}$ is equal to that of M on the edge e_1 and to 0 on the other edges from the construction of Υ_1.

By Lemma 5.3, on the edges of the triangle,

$$\begin{aligned} \frac{\partial \tilde{M}}{\partial x} &= \Upsilon_{1,x} M + \Upsilon_1 M_x \\ &= \Upsilon_1 M_x. \end{aligned}$$

Since Υ_1 vanishes on e_2 and e_3 and is equal to 1 on e_1, we find that $\nabla(M\Upsilon_1) = \nabla M$ on the edge e_1 and that it vanishes on the other edges.

By Lemma 5.2, we can bound $|\frac{\partial \tilde{M}}{\partial x}|$ as

$$\begin{aligned} \left|\frac{\partial \tilde{M}}{\partial x}\right| &\leq |\Upsilon_{1,x} M| + |\Upsilon_1 M_x| \\ &\leq \frac{C}{r} r + C \\ &\leq C. \end{aligned}$$

Similarly, we have $|\frac{\partial \tilde{M}}{\partial y}| \leq C$.

If we use Lemma 5.3 again, we find that

$$\begin{aligned}\left|\frac{\partial^2 \tilde{M}}{\partial x^2}\right| &\leq |\Upsilon_{1,xx} M| + 2|\Upsilon_{1,x} M_x| + |\Upsilon_1 M_{xx}| \\ &\leq \frac{C}{r^2} r + \frac{C}{r} + C \\ &\leq \frac{C}{r}.\end{aligned}$$

Similarly, we have $|\frac{\partial^2 \tilde{M}}{\partial x \partial y}| \leq \frac{C}{r}$ and $|\frac{\partial^2 \tilde{M}}{\partial y^2}| \leq \frac{C}{r}$. □

LEMMA 5.5. *For a given vertex v_i, let e_j, e_k be the two edges adjacent to v_i. Let us assume that M_j and M_k are C^2 functions on the closure of the triangle and that they go to 1 at least linearly at v_i. We also assume that M_j goes to 0 linearly at the other vertex of e_j and that M_k goes to 0 linearly at the other vertex of e_k. Let $\tilde{M} := \Upsilon_j M_j + \Upsilon_k M_k$. Then, $\nabla \tilde{M}$ is bounded by a constant and the second order partial derivatives of $\tilde{M}$ are bounded by $\frac{C}{r}$, where r is the minimum distance to the vertices of the triangle. The value of $\tilde{M}$ is equal to the value of M_j on the edge e_j, to the value of M_k on e_k and vanishes on the third edge. The gradient of $\tilde{M}$ is equal to the gradient of M_j on the edge e_j, to the gradient of M_k on the edge e_k and vanishes on the other edge.*

Proof. Without loss of generality, we can assume that j=1, k=2 and i=3. Let us define a linear function M_3 which vanishes on the edge e_3 and is equal to 1 at v_3.

If we use the fact that $1 = \Upsilon_1 + \Upsilon_2 + \Upsilon_3$, we can express $\tilde{M}$ as

$$\begin{aligned}\tilde{M} &= \Upsilon_1 M_1 + \Upsilon_2 M_2 \\ &= \Upsilon_1 M_1 + \Upsilon_2 M_2 - M_3 + M_3 \\ &= \Upsilon_1 (M_1 - M_3) + \Upsilon_2 (M_2 - M_3) - \Upsilon_3 M_3 + M_3.\end{aligned}$$

If we apply Lemma 5.4 to $\Upsilon_1(M_1 - M_3)$, $\Upsilon_2(M_2 - M_3)$ and $\Upsilon_3 M_3$, and add M_3 to the terms, we then can complete the proof. □

We define a displacement vertex basis function $w^0_{v_k}$ by giving the value 1 for w at one of the subdomain vertices, 0 at the others, and making it linear on the edges of the subdomain. In addition to the definition of w on the interface, we give values for θ_i on the two edges of the subdomain vertex being considered such that $\theta = \frac{1}{\ell_j} \mathbf{t} \psi_{e_j}$ where ℓ_j is the length of the edge, $\mathbf{t}$ is the unit tangent vector of an edge adjacent to our chosen subdomain vertex, and ψ_{e_j} is the edge cut-off function. The edge cut-off function is a piecewise linear function defined on the edge and has values 1 on all nodes except at the two ends of the edge where the cut-off function vanishes. Note that we make the value 0 to θ at the subdomain vertices for continuity.

LEMMA 5.6. *The Reissner-Mindlin energy of the vertex basis function $w^0_{v_k}$ is bounded by $\frac{C\tilde{m}}{H^2}(1 + log\frac{H}{h})$ where C does not depend on H, h, and δ, but depends on the shape regularity of the elements.*

Proof. Let us assume that the lengths of three edges of a subdomain are ℓ_1, ℓ_2, and ℓ_3 and that their relative lengths are bounded; this follows from the shape regularity of the elements. We first prove the lemma for $w^0_{v_1}$ using notation as in Figure 5.1.

Let us assume that the vertex basis function has the value 1 at the vertex v_1, and that the two edges e_2, e_3 of that vertex can be expressed by $a_2 x + b_2 y = c_2$ and $a_3 x + b_3 y = c_3$ respectively. (a_2, b_2) is the unit tangent vector of the edge e_2 from

The boundary values of the w component of $w^0_{v_1}$ on e_3. The height is 1.

The boundary values of the w component of $w^0_{v_1}$ on e_2. The height is 1.

The boundary values of the θ components of $w^0_{v_1}$ on e_3. The heights depends on $\mathbf{t}$ and ℓ_1.

The boundary values of the θ components of $w^0_{v_1}$ on e_2. The heights depend on $\mathbf{t}$ and ℓ_2.

The boundary values of θ and w vanish on the edge e_1.

FIG. 5.3. *Values of $w^0_{v_1}$ on the interface.*

v_3 to v_1, and (a_3, b_3) is the unit tangent vector of the edge e_3 from v_2 to v_1 and let (a_i', b_i') be the unit normal vector of the edge e_i.
Let again ξ_1, ξ_2, ξ_3 be the values of barycentric functions of the subdomain at (x, y). Let

$$w_i = \frac{\frac{1}{\xi_i^2}}{\frac{1}{\xi_1^2} + \frac{1}{\xi_2^2} + \frac{1}{\xi_3^2}} (\frac{a_i}{\ell_i} x + \frac{b_i}{\ell_i} y + c_i)$$

for i=2,3, where c_i is chosen so that the equation $\frac{a_i}{\ell_i} x + \frac{b_i}{\ell_i} y + c_i = 1$ at our chosen vertex v_1. Further, let $w = w_1 + w_2$. From Lemma 5.5, we know that w satisfies the boundary condition prescribed by the definitions of the basis function given above. We also know that the gradient of w is bounded by $\frac{C}{H}$ and that the second derivatives of w are bounded by $\frac{C}{Hr}$ where r is the minimum distance to the vertices.
Then, define $w_h = \widetilde{I^h}(w)$ and $\theta_L = I^h(\nabla w)$ on each element of the subdomain except in the elements next to each vertex where θ_L is defined by the linear components of θ. Here $\widetilde{I^h}$ is the standard second order interpolation operator and I^h is the standard first order interpolation operator. We can easily find bubble functions from the equation $\Pi\theta = \nabla w$ on each element. Because the scaling does not affect the H^1-seminorm and there are a bounded number of elements next to any vertex because of the shape regularity, we can bound the a-seminorm of the basis function on the elements next to the vertices easily as in Lemma 5.1.
For each element K which does not touch a subdomain vertex, we have

$$|\theta_L|^2_{H^1(K)} \leq |\nabla^2 w|^2_{H^1(K)}.$$

Therefore,

$$\begin{aligned} |\theta_L|^2_{H^1(\Omega_i)} &\leq C \int_0^{2\pi} \int_{ch}^{H} \frac{1}{H^2 r^2} r dr d\theta \ + \ C \\ &\leq \frac{C}{H^2}(1 + log\frac{H}{h}) \ + \ C. \end{aligned}$$

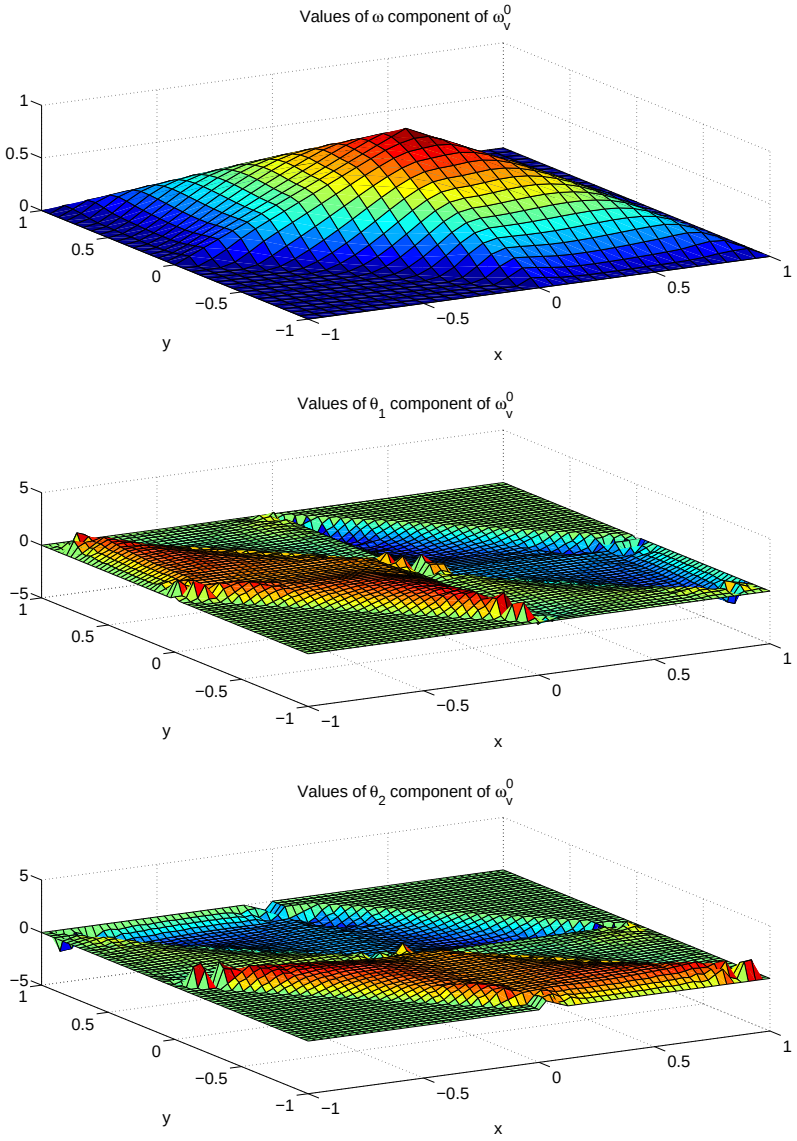

FIG. 5.4. *3d plot of the w vertex basis function* w_v^0.

For the bubble function θ_B, we know that

$$\Pi\theta_B = \nabla w_h - \theta_L = \nabla(\widetilde{I^h w}) - I^h(\nabla w) = \nabla(\widetilde{I^h w} - w) + (\nabla w - I^h(\nabla w)).$$

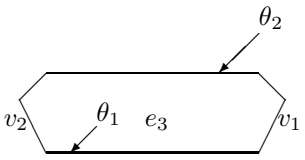

Boundary values of θ of $\theta^0_{e_3}$ on e_3.
All other boundary values of θ and w of $\theta^0_{e_3}$ are 0.

FIG. 5.5. *Values of $\theta^0_{e_3}$ on the interface.*

Therefore for each element K, which does not touch a subdomain vertex,

$$\begin{aligned}
|\theta_B|^2_{H^1(K)} &\leq \frac{C}{h^2}||\theta_B||^2_{L^2(K)} \\
&\leq \frac{C}{h^2}(||\nabla(\widetilde{I^h}w - w)||^2_{L^2(K)} + ||\nabla w - I^h(\nabla w)||^2_{L^2(K)}) \\
&\leq C(||\nabla(\widetilde{I^h}w - w)||^2_{L^\infty(K)} + ||\nabla w - I^h(\nabla w)||^2_{L^\infty(K)}) \\
&\leq Ch^2||\nabla^2 w||^2_{L^\infty(K)} \\
&\leq C\frac{h^2}{H^2 r^2}.
\end{aligned}$$

There are on the order of $\frac{H^2}{h^2}$ elements in each subdomin and the number of elements with a distance r from a vertex is about $\frac{r}{h}$. Therefore, to bound $|\theta_B|^2_{H^1(\Omega_i)}$, we need to estimate

$$C\sum_{i=1}^{\frac{H}{h}} \frac{1}{H^2}\frac{ih}{h}\frac{h^2}{i^2h^2} = C\sum_{i=1}^{\frac{H}{h}} \frac{1}{H^2}\frac{h}{ih}$$

where $r = ih$. This sum is bounded by $\frac{C}{H^2}(1 + log\frac{H}{h})$.

In total, the square of the H^1-seminorm of the function in the proof is bounded by $\frac{C}{H^2}(1 + log\frac{H}{h})$. Because we choose θ and w such that $\Pi\theta = \nabla w$, we can bound the Reissner-Mindlin energy by $\frac{C\tilde{m}}{H^2}(1 + log\frac{H}{h})$.

We can prove similar bounds for $w^0_{v_2}$ and $w^0_{v_3}$. ∎

We define a rotational edge basis function $\theta^0_{e_k}$ for each edge e_k by prescribing $\theta = \mathbf{n}\psi_{e_k}$ where $\mathbf{n}$ is the unit normal vector of the edge e_k pointing into the right half plane, and ψ_{e_k} is the edge cut-off function. We set all the boundary values of w to zero.

LEMMA 5.7. *The Reissner-Mindlin energy of the edge basis function $\theta^0_{e_k}$ is bounded by $C\tilde{m}(1 + log\frac{H}{h})$ where C does not depend on H, h, and δ, but depends on the shape regularity of the elements of the subdomain.*

Proof. We have the same assumptions as in the proof of Lemma 5.6. Consider

$$w_k := \frac{\frac{1}{\xi_k^2}}{\frac{1}{\xi_1^2} + \frac{1}{\xi_2^2} + \frac{1}{\xi_3^2}}(a'_k x + b'_k y + c'_k)$$

where c'_k is chosen so that $w_k = 0$ on the edge e_k. As in Lemma 5.6, we can prove that the square of the H^1-seminorm of the function is bounded by $C(1 + log(\frac{H}{h}))$ using

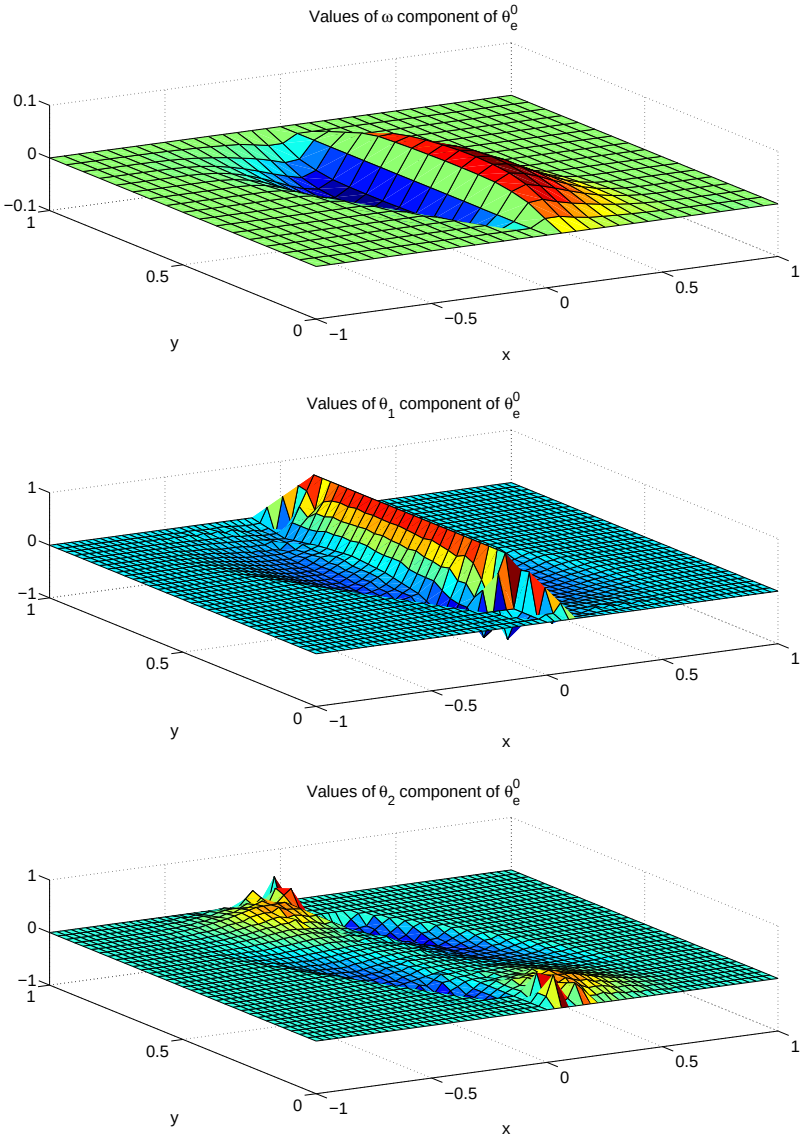

FIG. 5.6. *3d plot of the θ edge basis function θ_e^0.*

Lemma 5.4 instead of Lemma 5.5. □

In total, we have 9 vertex basis functions and 3 edge basis functions. Therefore, on average, we have 3 basis functions for each subdomain.

We now define a coarse interpolant u^0 by

$$u_0 = \sum_{i=1}^{3} w(v_i) w^0_{v_i} + \sum_{i=1}^{2}\sum_{j=1}^{3} \theta_i(v_j)\theta^0_{i,v_j} + \sum_{k=1}^{3} \frac{\int_{e_k} \theta \cdot \mathbf{n}}{\ell_{e_k}} \theta^0_{e_k} \tag{5.11}$$

where $\mathbf{n}$ is the unit normal vector of the boundary of the subdomain pointing into the right half plane. We can easily check that this coarse interpolant reproduces all functions in the null space of the Reissner-Mindlin energy and thus satisfies the null space property, cf. [31].

From [33, remark 4.13], we know that

$$||u||^2_{L^\infty(\Omega_i)} \leq C(1 + log\frac{H}{h})||u||^2_{H^1(\Omega_i)}, \qquad u \in H^1(\Omega_i) \cap V. \tag{5.12}$$

And it is easy to prove that

$$||u||^2_{L^2(\varepsilon)} \leq 2H||u||^2_{H^1(\Omega_i)}$$

where ε is an edge and that

$$\int_\varepsilon \frac{u \cdot n}{\ell} \leq C\sqrt{\int_\varepsilon \frac{u^2}{H^2}}\sqrt{H} \leq C\frac{||u||_{L^2_\varepsilon}}{\sqrt{H}} \leq C\sqrt{2}||u||_{H^1(\Omega_i)}. \tag{5.13}$$

Using inequalities (5.12) and (5.13) and Lemmas 5.1, 5.6 and 5.7 of this section to bound the energy of the coarse interpolant (5.11), we obtain the following bound:

$$a(u_0, u_0)_{\Omega_i} \leq \frac{C\tilde{m}}{H^2}(1 + log\frac{H}{h})^2||w||^2_{H^1(\Omega_i)} + C\tilde{m}(1 + log\frac{H}{h})^2||\theta||^2_{H^1(\Omega_i)}.$$

Using the equation $\nabla w = \Pi\theta$, we can show that

$$\frac{||\nabla w||^2_{L^2}}{H^2} \leq \frac{4||\theta||^2_{L^2}}{H^2}.$$

Because u^0 reproduce all the null space functions, we can use a Poincaré inequality by shifting by some null space functions and find that

$$\begin{aligned} a(u_0, u_0)_{\Omega_i} &\leq \frac{C\tilde{m}}{H^2}(1 + log\frac{H}{h})^2||w||^2_{H^1(\Omega_i)} + C\tilde{m}(1 + log\frac{H}{h})^2||\theta||^2_{H^1(\Omega_i)} \\ &\leq C\tilde{m}(1 + log\frac{H}{h})^2|\theta|^2_{H^1(\Omega_i)}. \end{aligned} \tag{5.14}$$

LEMMA 5.8. *Under the condition of $\Pi\theta = \nabla w$, the a-seminorm and the H^1-seminorm are equivalent for θ. This equivalence does not depend on H, h but depends on the shape regularity of elements and the Lamé constants. In particular, we have the relation $|\theta|^2_{H^1(\Omega_i)} \leq \frac{C}{\mu} a(\theta, \theta)$*

Proof. We can prove this lemma on each element of diameter h. Let us consider one element only and assume that one of its nodes is at (0,0). Then, we can use the following transformation to the reference element:

$$\begin{aligned} \tilde{w}(x, y) &= \frac{1}{h}(w(hx, hy) - w(0, 0)) + w(0, 0) \\ \tilde{\theta}(x, y) &= \theta(hx, hy). \end{aligned}$$

Then, $\nabla\tilde{w}(x,y) = \nabla w(hx,hy) = \Pi\theta(hx,hy) = \Pi\tilde{\theta}(x,y)$ on the reference element. We can easily see that the a-seminorm and the H^1-seminorm are invariant under this dilation. Therefore, it is enough to prove the lemma on the reference element.

On each element, we have 12 basis functions for θ. Among them are three null basis functions for $a(\theta,\theta)$ and two null basis functions for the H^1 norm. Two of these null basis functions are common. The remaining null basis function for $a(\theta,\theta)$ is $(-y,x)$ and this is not a valid basis function for this problem because of the condition $\nabla w = \Pi\theta$.

Because we consider a finite dimensional problem and the null space of the two seminorms are the same, the two seminorms are equivalent and we get the bound $|\theta|^2_{H^1(\Omega_i)} \leq \frac{C}{\mu}a(\theta,\theta)$. □

Using Lemma 5.8 and inequality (5.14), we can prove that

$$a(u^0,u^0) \leq C\frac{\tilde{m}}{\mu}(1+log\frac{H}{h})^2 a(u,u). \tag{5.15}$$

We note that if the material becomes more incompressible, the decomposition becomes less stable.

If $\partial\Omega_i \bigcap \partial\Omega \neq \emptyset$ with a strictly positive measure, we can define similar basis functions except on $\partial\Omega$. In such subdomain, we can prove a bound of the square of the a-seminorm by using a Friedrichs inequality.

If $\partial\Omega_i$ intersects $\partial\Omega$ only at one or a few points, we need to modify the proof. Let us assume that $\partial\Omega_i$ intersects $\partial\Omega$ at (0,0). Let us find $ax+by+c$ such that $a = \int_{\Omega_i}\theta_1$, $b = \int_{\Omega_i}\theta_2$ and $c = \int_{\Omega_i}(w-ax-by)$. Because θ_1 vanishes at a point, we have that

$$\begin{aligned}
||\theta_1||_{L^\infty(\Omega_i)} &\leq ||\theta_1 - a||_{L^\infty(\Omega_i)} + |a| \\
&\leq 2||\theta_1 - a||_{L^\infty(\Omega_i)} \\
&\leq C\sqrt{1+log\frac{H}{h}}||\theta_1 - a||_{H^1(\Omega_i)} \\
&\leq C\sqrt{1+log\frac{H}{h}}|\theta_1|_{H^1(\Omega_i)}
\end{aligned} \tag{5.16}$$

which is a variation of inequality (5.12). Similarly, we have

$$||\theta_2||^2_{L^\infty(\Omega_i)} \leq C(1+log\frac{H}{h})|\theta_2|^2_{H^1(\Omega_i)} \tag{5.17}$$

We also have that

$$\int_\varepsilon \frac{\theta\cdot n}{\ell} \leq C||\theta||_{L^\infty(\Omega_i)} \leq C\sqrt{1+log\frac{H}{h}}|\theta|_{H^1(\Omega_i)}. \tag{5.18}$$

which is a variation of inequality (5.13).

For w,

$$\begin{aligned}
||w||_{L^\infty(\Omega_i)} &\leq ||w-ax-by-c||_{L^\infty(\Omega_i)} + |c| + ||ax+by||_{L^\infty(\Omega_i)} \\
&\leq 2||w-ax-by-c||_{L^\infty(\Omega_i)} + (|a|+|b|)H \\
&\leq C\sqrt{1+log\frac{H}{h}}||w-ax-by-c||_{H^1(\Omega_i)} + (|a|+|b|)H \\
&\leq C\sqrt{1+log\frac{H}{h}}|w-ax-by-c|_{H^1(\Omega_i)} + (|a|+|b|)H.
\end{aligned} \tag{5.19}$$

Using the equation $\nabla(w - ax - by - c) = \Pi(\theta - (a, b))$, we can show that

$$||\nabla(w - ax - by - c)||^2_{L^2(\Omega_i)} \leq 4||\theta - (a, b)||^2_{L^2(\Omega_i)}.$$

The first term of (5.19) is bounded by

$$C\sqrt{1 + log\frac{H}{h}}||\theta - (a, b)||_{L^2(\Omega_i)} \leq CH\sqrt{1 + log\frac{H}{h}}|\theta|_{H^1(\Omega_i)}$$

by the Poincaré inequality.

$$|a| \leq H^2||\theta_1||_{L^\infty(\Omega_i)} \leq CH^2\sqrt{1 + log\frac{H}{h}}|\theta_1|_{H^1(\Omega_i)}$$

We can obtain similar bound for $|b|$ and

$$||w||_{L^\infty(\Omega_i)} \leq CH\sqrt{1 + log\frac{H}{h}}|\theta|_{H^1(\Omega_i)}. \tag{5.20}$$

Using Lemmas 5.1, 5.6 and 5.7 of this section and inequalities (5.16), (5.17), (5.20) and (5.18) instead of (5.12) and (5.13), we obtain the following bound:

$$a(u^0, u^0) \leq C\tilde{m}(1 + log\frac{H}{h})^2|\theta|^2_{H^1(\Omega_i)}. \tag{5.21}$$

Using Lemma 5.8 and inequality (5.21), we can prove that

$$a(u^0, u^0) \leq C\frac{\tilde{m}}{\mu}(1 + log\frac{H}{h})^2 a(u, u). \tag{5.22}$$

Remark. We can also define a w edge basis function on each edge. These basis functions are not necessary in our proof, however they make the constant in decomposition smaller. We will compare numerical results with such w edge basis functions with results without them in section 8. In our experiments, the condition numbers of the preconditioned system with these additional basis functions are much smaller than those without.

On each edge of a subdomain, we prescribe the values of a quadratic which vanishes at the two subdomain vertices of the edge and has a maximum of 1 on the edge. In addition to the definition of w on the interface, we give values for θ in the subdomain such that $\theta = (\mathbf{t} \cdot \nabla w)\mathbf{t}\psi_{e_k}$ where $\mathbf{t}$ is the unit tangent vector of the edge and ψ_{e_k} is the edge cut-off function. We denote these basis functions by $w^0_{e_k}$, k=1,2,3.

LEMMA 5.9. *The Reissner-Mindlin energy of the edge basis function $w^0_{e_k}$ is bounded by $\frac{C\tilde{m}}{H^2}(1 + log\frac{H}{h})$ where C does not depend on H, h, and δ, but depends on the shape regularity of the elements of the subdomain.*

Proof. We have the same assumptions as in the proof of Lemma 5.6. w_i is defined by $\frac{\frac{1}{\xi_i^2}}{\frac{1}{\xi_1^2}+\frac{1}{\xi_2^2}+\frac{1}{\xi_3^2}}g(x, y)$ where $g(x, y)$ is the second order polynomial of (x, y) chosen so that $g(x, y)$ is 1 at the midpoint of the edge being considered and vanishes at all vertices and midpoints of the other edges. $g(x, y)$ is the standard basis function in P_2 with the midpoint node. As in Lemma 5.6, we can prove that the square of the H^1-seminorm of this function is bounded by $\frac{C}{H^2}(1 + log\frac{H}{h})$ using Lemma 5.4 instead of Lemma 5.5. □

Similarly, we can define θ edge basis functions related to the normal direction. But they did not give much improvement in our numerical experiments.

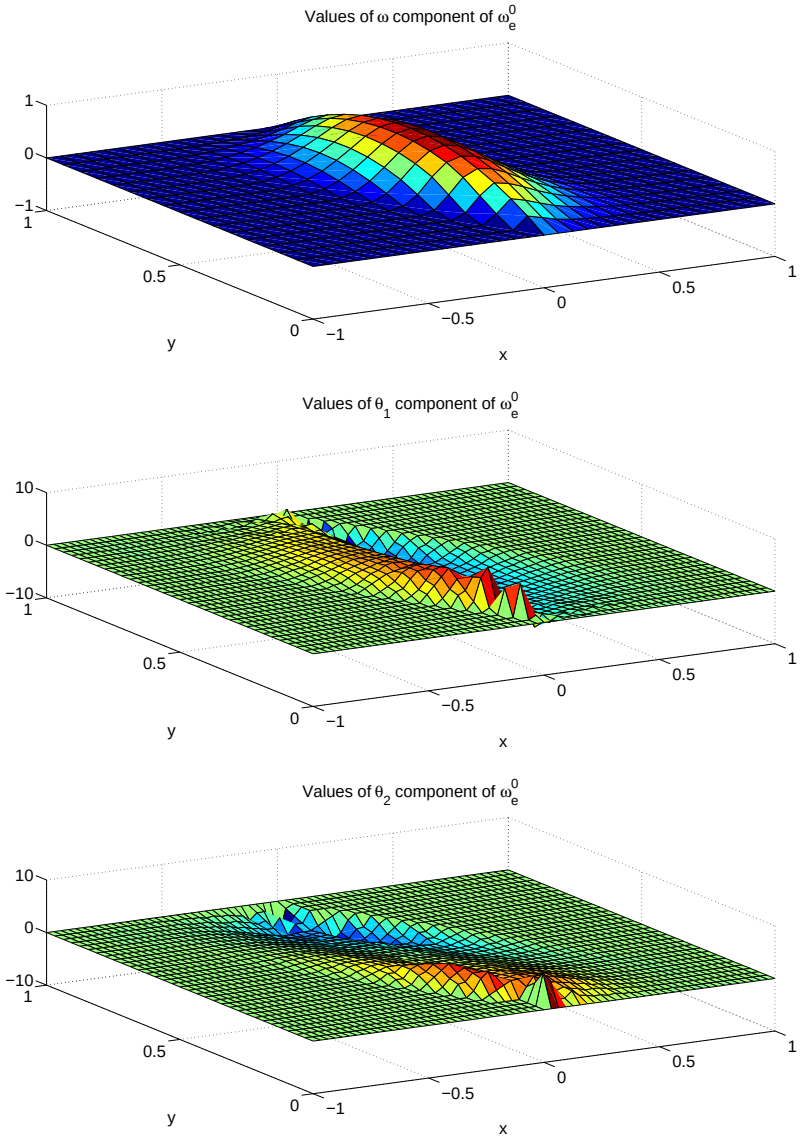

FIG. 5.7. *3d plot of the w edge basis function* w_e^0.

5.3.2. Local Problems. Let $w_d = w - w^0$, $\theta_{dL} = \theta_L - \theta_L^0$ and $\Pi\theta_{dB} = \nabla w_d - \theta_{dL}$. Then, $\Pi\theta_d = \theta_{dL} + \Pi\theta_{dB} = \nabla w_d$.
From Lemma 5.8 and inequality (5.15), we know that

$$|\theta_d|^2_{H^1(\Omega_i)} \leq C\frac{\tilde{m}}{\mu^2}(1 + log\frac{H}{h})^2 a(u,u)_{\Omega_i}. \tag{5.23}$$

If we use the Friedrichs inequality, we obtain

$$||\theta_d||^2_{L^2(\Omega_i)} \leq C\frac{\tilde{m}}{\mu^2}(1+log\frac{H}{h})^2 H_i^2 a(u,u)_{\Omega_i}. \tag{5.24}$$

From the equation $\Pi\theta = \nabla w$, we have the inequality $||\nabla w||^2_{L^2(\Omega_i)} \leq ||\theta||^2_{L^2(\Omega_i)}$. Therefore,

$$||w_d||^2_{H^1(\Omega_i)} \leq C\frac{\tilde{m}}{\mu^2}(1+log\frac{H}{h})^2 H_i^2 a(u,u)_{\Omega_i}. \tag{5.25}$$

Similarly,

$$||w_d||^2_{L^2(\Omega_i)} \leq C\frac{\tilde{m}}{\mu^2}(1+log\frac{H}{h})^2 H_i^4 a(u,u)_{\Omega_i}. \tag{5.26}$$

Let χ_j be nonnegative C^∞ functions in $\mathbb{R}^2$ such that

$$\begin{aligned} \chi_j &= 0 \text{ on } \Omega\backslash\Omega_j \\ \sum_{j=1}^{N}\chi_j &= 1 \text{ on } \overline{\Omega} \\ ||\nabla\chi_j||_{L^\infty} &\leq C\delta_i^{-1} \\ ||\nabla^2\chi_j||_{L^\infty} &\leq C\delta_i^{-2}. \end{aligned}$$

The construction of χ_j is standard, cf, e.g., [11].

We define the local components of the Schwarz decomposition as follows: $w_j := \widetilde{I^h}(\chi_j w_d)$ and $\theta_{Lj} := I^h(\chi_j\theta_{dL} + w_d\nabla\chi_j)$. Here $\widetilde{I^h}$ is the standard interpolator onto the piecewise quadratic continuous functions on each element and I^h is the standard interpolator onto the piecewise linear continuous functions on each element as in Lemma 5.6. Because $\sum\chi_j = 1$ and $\sum\nabla\chi_j = 0$, the above formulas provide a decomposition. For the bubble functions, we use the condition $\nabla w = \Pi\theta$.
Given $\delta_i > 0$, let $\Omega_{i,\delta_i} \subset \Omega_i'$ be the set of points that are within a distance δ of $\partial\Omega_i' \setminus \partial\Omega$. Let $B(\Omega_i)$ be the union of the subdomains which intersect Ω_i. We need to use [33, lemma 3.10].

LEMMA 5.10. *There exist a constant C such that*

$$\begin{aligned} ||u||^2_{L^2(\Omega_{i,\delta_i})} &\leq C\delta_i^2(1+\frac{H_i}{\delta_i})||u||^2_{H^1(\Omega_i')} \\ &\leq C\delta_i^2(1+\frac{H_i}{\delta_i})||u||^2_{H^1(B(\Omega_i))}. \end{aligned}$$

We know that derivatives of χ_j are nonzero only in a δ-neighborhood of the boundary of subdomains. We find using (5.23), (5.24), (5.25) and (5.26), that

$$
\begin{aligned}
|\theta_{Lj}|^2_{H^1(\Omega_i)} &\le ||\nabla I^h(\chi_j\theta_{dL}+w_d\nabla\chi_j)||^2_{L^2(\Omega_i)}\\
&\le ||\nabla(\chi_j\theta_{dL}+w_d\nabla\chi_j)||^2_{L^2(\Omega_i)}\\
&\le C(||\theta_{dL}\nabla\chi_j||^2_{L^2(\Omega_i)}+||\chi_j\nabla\theta_{dL}||^2_{L^2(\Omega_i)}+\\
&\quad ||w_d\nabla^2\chi_j||^2_{L^2(\Omega_i)}+||\nabla\chi_j\nabla w_d||^2_{L^2(\Omega_i)})\\
&\le C(\frac{1}{\delta_i^2}||\theta_{dL}||^2_{L^2(\Omega_i)}+||\nabla\theta_{dL}||^2_{L^2(\Omega_i)}+\\
&\quad \frac{1}{\delta_i^4}||w_d||^2_{L^2(\Omega_{i,\delta_i})}+\frac{1}{\delta_i^2}||\nabla w_d||^2_{L^2(\Omega_i)})\\
&\le C(\frac{1}{\delta_i^2}||\theta_d||^2_{L^2(\Omega_i)}+||\nabla\theta_d||^2_{L^2(\Omega_i)}+\\
&\quad \frac{1}{\delta_i^2}(1+\frac{H_i}{\delta_i})||w_d||^2_{H^1(B(\Omega_i))}+\frac{1}{\delta_i^2}||w_d||^2_{H^1(\Omega_i)})\\
&\le C\frac{\tilde{m}}{\mu^2}\Big((1+log\frac{H}{h})^2\frac{H_i^2}{\delta_i^2}a(u,u)_{\Omega_i}+(1+log\frac{H}{h})^2a(u,u)_{\Omega_i}\\
&\quad (1+log\frac{H}{h})^2(1+\frac{H}{\delta})^3a(u,u)_{B(\Omega_i)}+(1+log\frac{H}{h})^2(\frac{H}{\delta})^2a(u,u)_{\Omega_i}\Big)\\
&\le C\frac{\tilde{m}}{\mu^2}(1+\frac{H_i}{\delta_i})^3(1+log\frac{H}{h})^2a(u,u)_{B(\Omega_i)}. \qquad (5.27)
\end{aligned}
$$

For the bubble functions on each element, we have

$$
\begin{aligned}
|\theta_{Bj}|^2_{H^1(K)} &\le \frac{C}{h^2}||\theta_{Bj}||^2_{L^2(K)}\\
&\le \frac{C}{h^2}||\nabla w_j-\theta_{Lj}||^2_{L_2(K)}\\
&\le \frac{C}{h^2}||\nabla(\widetilde{I^h}(\chi_j w_d))-I^h(\chi_j\theta_{dL}+w_d\nabla\chi_j)||^2_{L^2(K)}\\
&\le \frac{C}{h^2}||\nabla(\widetilde{I^h}(\chi_j w_d))-\nabla(\chi_j w_d)+\nabla(\chi_j w_d)-I^h(\chi_j\theta_{dL}+w_d\nabla\chi_j)||^2_{L^2(K)}\\
&\le \frac{C}{h^2}||\nabla(\widetilde{I^h}(\chi_j w_d))-\nabla(\chi_j w_d)||^2_{L^2(K)}+\frac{C}{h^2}||\chi_j\nabla w_d-I^h(\chi_j\theta_{dL})||^2_{L^2(K)}\\
&\quad +\frac{C}{h^2}||w_d\nabla\chi_j-I^h(w_d\nabla\chi_j)||^2_{L^2(K)}. \qquad (5.28)
\end{aligned}
$$

The first term of (5.28) can be bounded by

$$
\begin{aligned}
&C||\nabla^2(\chi_j w_d)||^2_{L^2(K)}\\
&\le C||w_d\nabla^2\chi_j+2\nabla\chi_j\nabla w_d+\chi_j\nabla^2(w_d)||^2_{L^2(K)}\\
&\le C||w_d\nabla^2\chi_j||^2_{L^2(K)}+2||\nabla\chi_j\nabla w_d||^2_{L^2(K)}+||\chi_j\nabla\theta_d||^2_{L^2(K)}.
\end{aligned}
$$

If we add the above bound over the subdomain Ω_i, we then have

$$
\begin{aligned}
&\frac{C}{h^2}||\nabla(\widetilde{I^h}(\chi_j w_d))-\nabla(\chi_j w_d)||^2_{L^2(\Omega_i)}\\
&\qquad \le C(\frac{1}{\delta_i^4}||w_d||^2_{L^2(\Omega_{i,\delta_i})}+\frac{1}{\delta_i^2}||\nabla w_d||^2_{L^2(\Omega_{i,\delta_i})}+||\nabla\theta_d||^2_{L^2(\Omega_i)})\\
&\qquad \le C\frac{\tilde{m}}{\mu^2}(1+\frac{H_i}{\delta_i})^3(1+log\frac{H}{h})^2a(u,u)_{B(\Omega_i)}. \qquad (5.29)
\end{aligned}
$$

The second term of (5.28) is bounded similarly by

$$\begin{aligned}\frac{C}{h^2}||\chi_j\nabla w_d - I^h(\chi_j\theta_{dL})||^2_{L^2(K)}&\\ \leq \frac{C}{h^2}||\chi_j\nabla w_d - \chi_j\theta_{dL}||^2_{L^2(K)} + \frac{C}{h^2}||\chi_j\theta_{dL} - I^h(\chi_j\theta_{dL})||^2_{L^2(K)}&\\ \leq \frac{C}{h^2}||\chi_j\theta_{dB}||^2_{L^2(K)} + \frac{C}{h^2}||\chi_j\theta_{dL} - I^h(\chi_j\theta_{dL})||^2_{L^2(K)}&\\ \leq C|\theta_{dB}|^2_{H^1(K)} + C||\nabla(\chi_j\theta_{dL})||^2_{L^2(K)}.&\end{aligned}$$

Therefore, using the bound for the linear part of the θ in (5.29), we have

$$\frac{C}{h^2}||\chi_j\nabla w_d - I^h(\chi_j\theta_{dL})||^2_{L^2(\Omega_i)} \leq C\frac{\tilde{m}}{\mu^2}(1+\frac{H_i}{\delta_i})^3(1+log\frac{H}{h})^2a(u,u)_{B(\Omega_i)}. \quad (5.30)$$

We can bound the sum of the third term of (5.28) over Ω_i by $\frac{C}{\mu}(1+\frac{H_i}{\delta_i})^3(1+log\frac{H}{h})^2a(u,u)_{B(\Omega_i)}$.

In total, we have

$$\begin{aligned}\sum_{j=0}^{N} a(u_j,u_j)_{\Omega_i} &\leq C\tilde{m}\sum_{j=0}^{N}|\theta_j|^2_{H^1(\Omega_i)}\\ &\leq C\frac{\tilde{m}^2}{\mu^2}(1+\frac{H_i}{\delta_i})^3(1+log\frac{H}{h})^2a(u,u)_{B(\Omega_i)}.\end{aligned}$$

Summing over the subdomains, the decomposition is stable with the bound

$$C_0^2 \leq C(\frac{\tilde{m}}{\mu})^2(1+\frac{H}{\delta})^3(1+log\frac{H}{h})^2.$$

THEOREM 5.11. *In case exact solver are employed on all subspaces, the condition number of the additive Schwarz operator for sufficiently small t is bounded by*

$$C(\frac{\tilde{m}}{\mu})^2(1+\frac{H}{\delta})^3(1+log\frac{H}{h})^2$$

where C depends on N^c, but is otherwise independent of t, h, H, and δ.

5.4. The Case of t=∞.

5.4.1. Coarse Problem. If t=∞, the Reissner-Mindlin plate problem is just the linear elasticity problem. For more details, see [20].

We define basis functions on the interface and then use discrete harmonic extensions of these boundary values.

For each θ^i, we define a vertex basis function θ^0_{i,v_k} which is linear on each edge and has the value the 1 at a vertex.

LEMMA 5.12. *The square of the a-seminorm of the vertex basis function θ^0_{i,v_k} is bounded by $C\tilde{m}$ where C does not depend on H, h, and δ, but depends on the shape regularity of the elements of the subdomain.*

We define a coarse component u_0 of u by

$$u_0 = \sum_{j=1}^{2}\sum_{k=1}^{3}\theta_j(v_k)\theta^0_{j,v_k}.$$

This coarse interpolant reproduces both null space functions of θ of the a-seminorm. We have,

$$\begin{aligned} a(u_0,u_0)_{\Omega_i} &\leq C\tilde{m}||\theta||^2_{L^2(\Omega_i)} \\ &\leq C\tilde{m}(1+log\frac{H}{h})||\theta||^2_{H^1(\Omega_i)} \\ &\leq C\frac{\tilde{m}}{\mu}(1+log\frac{H}{h})a(u,u) \end{aligned}$$

by using Korn's inequality, see, e.g., [10], after replacing $||\theta||^2_{H^1(\Omega_i)}$ by $\inf_{r\in RB}||\theta - r||^2_{H^1(\Omega_i)}$.

5.4.2. Local Problems. Let $w_d = w - w^0$, $\theta_{dL} = \theta_L - \theta^0_L$. We define the local components as follows; $w_j := \widetilde{I^h}(\chi_j w_d)$ and $\theta_{Lj} := I^h(\chi_j\theta_{dL})$. Because $\sum\chi_j = 1$ and $\sum\nabla\chi_j = 0$, the above formulas provide a decomposition. We find

$$\begin{aligned} a(\theta_j,\theta_j)_{\Omega_i} &\leq C\tilde{m}|\theta_j|^2_{H^1(\Omega_i)} \\ &\leq C\tilde{m}||\nabla I^h(\chi_j\theta_d)||^2_{L^2(\Omega_i)} \\ &\leq C\tilde{m}(||\theta_d\nabla\chi_j||^2_{L^2(\Omega_i)} + ||\chi_j\nabla\theta_d||^2_{L^2(\Omega_i)} \\ &\leq C\tilde{m}(\frac{1}{\delta^2}||\theta_d||^2_{L^2(\Omega_i,\delta)} + ||\nabla\theta_d||^2_{L^2(\Omega_i)}) \\ &\leq C\tilde{m}(1+\frac{H}{\delta})||\theta_d||^2_{\Omega_i} \\ &\leq C\tilde{m}(1+\frac{H}{\delta})(1+log\frac{H}{h})||\theta||^2_{\Omega_i} \end{aligned}$$

by Lemma 5.10. By replacing $||\theta||^2_{H^1(\Omega_i)}$ by $\inf_{r\in RB}||\theta - r||^2_{H^1(\Omega_i)}$, we obtain

$$\begin{aligned} a(\theta_j,\theta_j)_{\Omega_i} &\leq C\frac{\tilde{m}}{\mu}(1+\frac{H}{\delta})(1+log\frac{H}{h})||\theta||^2_{\Omega_i} \\ &\leq C\frac{\tilde{m}}{\mu}(1+\frac{H}{\delta})(1+log\frac{H}{h})a(\theta,\theta)_{\Omega_i}. \end{aligned}$$

The condition number is bounded by $C\frac{\tilde{m}}{\mu}(1+\frac{H}{\delta})(1+log\frac{H}{h})$.

If we do not include the coarse basis functions of this section, then the condition number of the additive operator grows rapidly with the number of subdomains for large t, like $t > 1$. When we added them in our numerical experiments, the additive method was quasi-optimal and scalable for any t, especially for large t. But it does not improve the condition number of the additive method for small t which are of more interest. The Reissner-Mindlin problem with large t does not have physical meaning and there is no strong reason for us to add unnecessary variable w to the linear elasticity problem. If we were to include these coarse basis functions, we need to deal with a larger coarse space and it would increase the computation time.

6. Changes of Thickness t or the Lamé constants. It is of interest to consider cases where the thickness and the Lamé parameters change across the domain. For simplicity, we assume that the thickness and the Lamé constants are piecewise constant. In this case, we can divide the domain into triangle subdomains such that

t, μ, λ are constants on each subdomain. We can see that the proof of previous sections does not depend on t, μ and λ if t and $\frac{\lambda}{\mu}$ are bounded from above. Therefore, we still get the same $C(\frac{\tilde{m}}{\mu})^2(1+log\frac{H}{h})^2(1+\frac{H}{\delta})^3$ bound even when t, μ and λ change over the domain.

7. Higher Order Falk-Tu Element. The kth order Falk-Tu elements are defined as follows; see [9], [23]:

$$\Theta_h = \boldsymbol{M}_{1,0}^{k-1} + \boldsymbol{B}^{k+2},\ W_h = M_{1,0}^k,\ \Gamma_h = \boldsymbol{M}_0^{k-1}.$$

Here $\boldsymbol{M}_{a,0}^k$ is the space of piecewise kth order polynomials in $\boldsymbol{H}_0^a(\Omega)$, $M_{a,0}^k$ the space of piecewise kth order polynomials in $H_0^a(\Omega)$, $\boldsymbol{M}_a^k$ the space of piecewise kth order polynomials in $\boldsymbol{H}^a$, and $\boldsymbol{B}^k$ the space of piecewise kth order bubble functions. So far, we have considered the case $k = 2$. Note that we again choose a discontinuous stress variable. The discrete problem is:
Find $\theta_h \in \Theta_h, w_h \in W_h$ such that

$$a(\theta_h, \phi) + \frac{\lambda}{t^2}(\nabla w_h - \Pi\theta_h, \nabla v - \Pi\phi) = (g, v) - (\boldsymbol{f}, \phi), \phi \in \Theta_h, v \in W_h$$

We have an error estimate similar to theorem 3.1. For a proof, see [9, pp213].

THEOREM 7.1. *For sufficiently smooth solutions of the continuous problem, we have for* $1 \le r \le k-1$

$$\|\theta - \theta_h\|_0 + \|w - w_h\|_1 \le Ch^{r+1}(||\theta||_{r+1} + ||w||_{r+2} + t||\gamma||_r + ||\gamma||_{r+1})$$

where C is independent of h.

We can decompose Θ_h into two parts, the polynomial θ_L and the bubble function θ_B. We then have $a(\theta_L+\theta_B, \theta_L+\theta_B) \ge C(a(\theta_L, \theta_L)+a(\theta_B, \theta_B))$ because we consider a finite dimensional space. We know that $\nabla W_h \subset \Pi\theta_B$ and $\theta_L \subset \theta_B$ and that $w = \Pi\theta$ implies that $||w||_{L^2}^2 \le ||\theta||_{L^2}^2$. Therefore, we can easily modify our proof for the higher order Falk-Tu element and obtain the same bound.

8. Numerical Experiments. In the numerical experiments, L is the length of one side of a square domain, ν, E and λ are the parameters of elasticity, H is the size of the coarse mesh, h that of the fine mesh, δ that of the overlap, and t the thickness of the plate. Results are given for the elasticity parameters $\nu = 0.8,\ E = 0.1,\ \lambda = 0.1$. Experiments for each parameter set is done about 100 times with random right hand sides and the average iteration counts and condition numbers are given. We use the additive method and the conjugate gradient algorithm to solve the linear system of equations. The stopping criteria for the CG algorithm is $\frac{||r_n||_{l^2}}{||r_0||_{l^2}} \le 10^{-7}$. We calculated the condition number by constructing a matrix of coefficients given by the conjugate gradient method as in O'Leary and Widlund, cf. [29].

The condition numbers as a function number of subdomains are given in Tables 8.1 and 8.2. As expected, the condition number grows with the number of subdomains for large t, but it is bounded for small t.

TABLE 8.1
Results for $L = 1$, $\frac{H}{h} = 4$, $\frac{H}{\delta} = 4$, and decreasing $h = \frac{1}{n}$, increasing the number of subdomains $= \frac{n}{4} \times \frac{n}{4}$ without the w quadratic coarse basis functions.

n	Iter	cond	Iter	cond	Iter	cond	Iter	cond
t	10		0.1		0.001		0.00001	
12	36.3	70.5	31.1	29.8	80.2	379.6	81.5	383.2
24	63.5	309.9	38.0	42.3	153.2	662.8	162.4	704.6
36	92.2	772.7	49.9	79.3	191.3	851.7	207.9	949.9
48	122.0	1492.8	61.1	114.3	208.0	767.0	233.1	1015.7
60	150.2	2500.6	73.0	171.6	208.0	746.9	251.5	972.2
72	179.9	3823.5	87.0	236.3	215.0	714.4	265.9	1022.1
84	208.7	5483.0	101.7	308.0	209.9	607.7	281.0	976.6

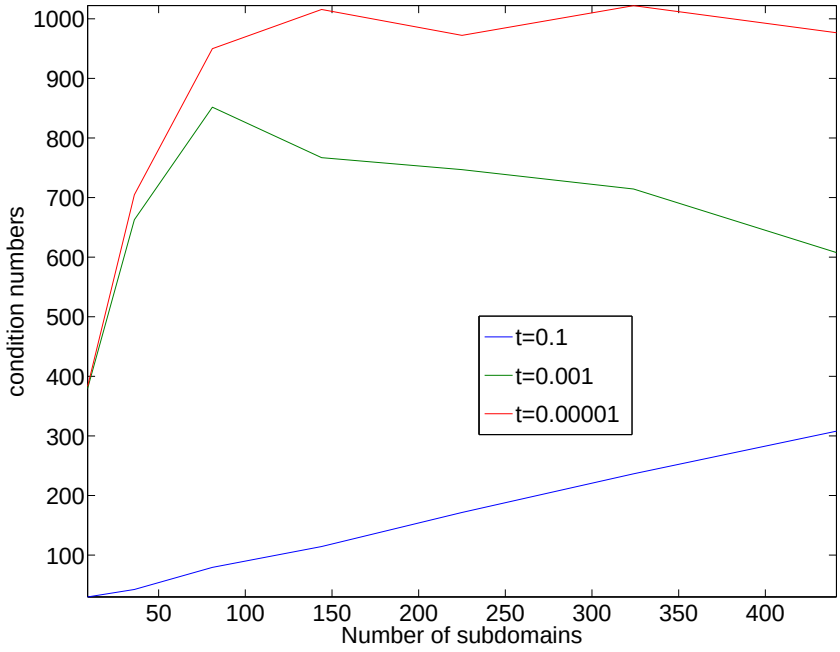

FIG. 8.1. *The condition numbers as a function of the number of subdomains without the w quadratic coarse basis functions.*

TABLE 8.2
Results for $L = 1$, $\frac{H}{h} = 4$, $\frac{H}{\delta} = 4$, and decreasing $h = \frac{1}{n}$, increasing the number of subdomains $= \frac{n}{4} \times \frac{n}{4}$ with the w quadratic coarse basis functions.

n	Iter	cond	Iter	cond	Iter	cond	Iter	cond
t	10		0.1		0.001		0.00001	
12	35.2	70.5	25.1	17.5	58.0	77.5	59.3	78.1
24	64.0	310.1	37.0	35.9	66.0	69.1	68.7	72.4
36	93.0	772.9	49.0	73.7	67.6	68.1	73.7	75.2
48	121.9	1494.3	60.8	107.2	67.0	64.4	75.0	76.3
60	151.2	2503.0	74.0	161.7	65.0	66.6	75.2	77.4
72	180.1	3826.3	87.1	220.6	64.0	65.4	76.9	77.5
84	209.7	5484.9	100.7	291.6	62.0	62.6	77.0	76.6

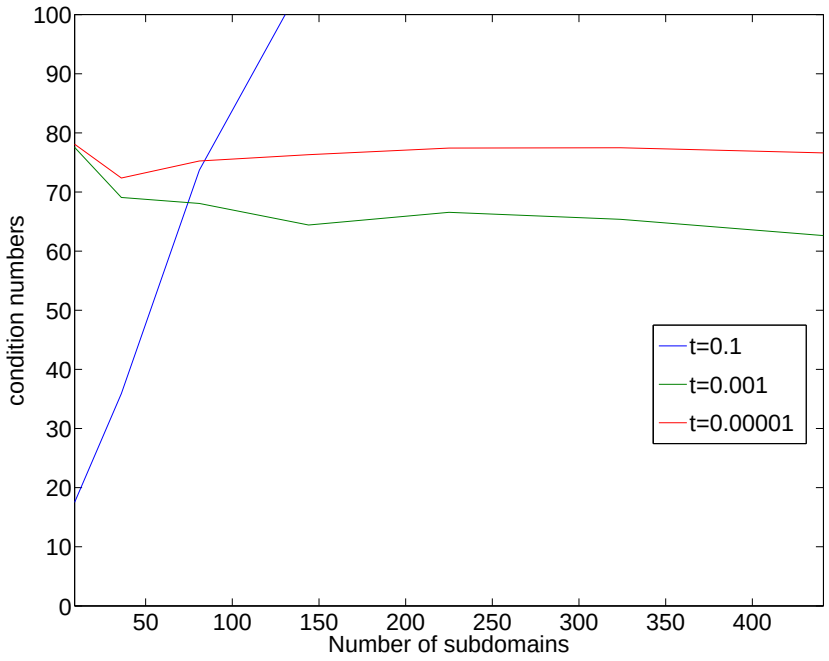

FIG. 8.2. *The condition numbers as a function of the number of subdomains with the w quadratic coarse basis functions.*

TABLE 8.3
Results for $L = 1,\ \frac{H}{h} = 4,\ \frac{H}{\delta} = 4$, *and decreasing* $h = \frac{1}{n}$, *increasing the number of subdomains* $= \frac{n}{12} \times \frac{n}{12}$.

$\frac{H}{h}$	Iter	cond	Iter	cond
t	100		10	
12	41.6	17.50	40.0	18.13
24	45.0	20.69	43.7	18.61
36	46.0	21.09	44.0	18.21
48	46.0	20.07	44.9	17.96
60	46.0	18.90	44.5	18.92
72	46.0	18.08	44.7	19.69
84	46.0	18.38	45.0	20.24
96	46.0	18.76	45.0	20.57

If we add more coarse basis functions for linear elasticity probelm, then we can get condition numbers that do not increase as the number of subdomains increases for large t. The results with the increased coarse space for large t are in Table 8.3. These results do not depend on the number of subdomains.

TABLE 8.4
Results are for $L = 1$, $h = \frac{1}{n}$, $\frac{H}{\delta} = 4$, the number of subdomains 3×3, and increasing $\frac{H}{h} = \frac{n}{3}$ without the w quadratic coarse basis functions.

$\frac{H}{h}$	Iter	cond	Iter	cond	Iter	cond	Iter	cond	Iter	cond
t	1000		10		0.1		0.001		0.00001	
4	38.9	69.1	36.2	70.5	31.1	29.7	80.2	379.0	81.3	386.2
8	45.5	66.3	40.7	67.2	32.9	28.8	80.0	284.0	80.8	299.9
12	45.8	64.2	41.8	64.1	33.7	31.1	79.5	307.5	80.4	337.4
16	46.1	64.4	42.5	65.1	34.3	31.8	79.2	313.9	80.0	358.0
20	46.9	62.8	43.2	63.7	34.5	31.9	79.0	301.4	81.6	361.3
24	47.4	62.9	43.5	64.0	34.6	33.4	79.0	288.1	89.2	354.4
28	47.7	63.3	43.6	64.4	35.0	34.4	79.2	268.8	89.6	345.3

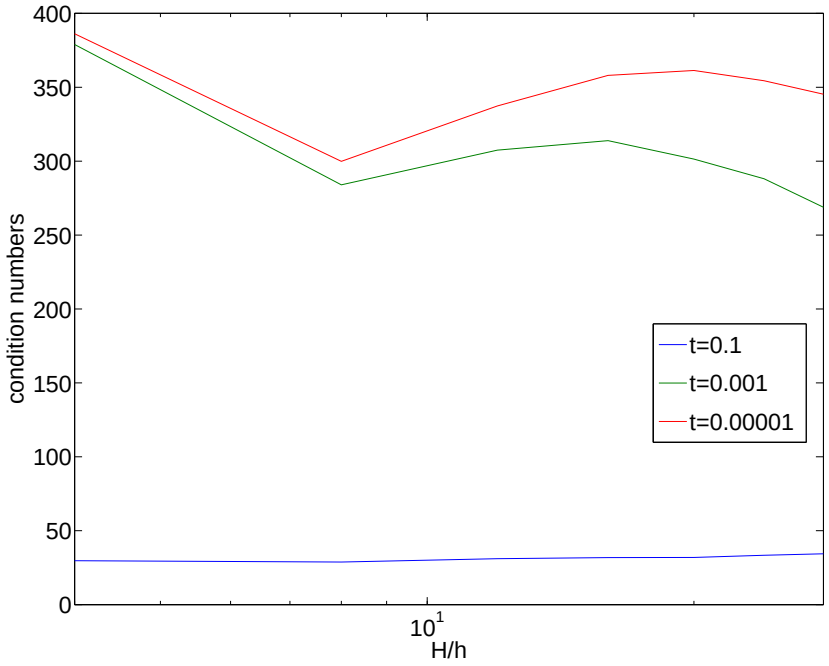

FIG. 8.3. *The condition numbers as a function of $\frac{H}{h}$ without the w quadratic coarse basis functions.*

Results with varying $\frac{H}{h}$ are given in Tables 8.4 and 8.5 and Figures 8.3 and 8.4.

TABLE 8.5

Results are for $L = 1,\ h = \frac{1}{n},\ \frac{H}{\delta} = 4$, the number of subdomains 3×3, and increasing $\frac{H}{h} = \frac{n}{3}$ with the w quadratic coarse basis functions.

$\frac{H}{h}$	Iter	cond	Iter	cond	Iter	cond	Iter	cond	Iter	cond
t	1000		10		0.1		0.001		0.00001	
4	39.0	69.4	35.2	70.4	25.1	17.5	58.0	78.1	59.1	79.0
8	46.2	65.6	41.6	66.1	28.0	17.2	59.5	79.0	61.9	82.5
12	47.0	65.5	42.6	63.9	29.4	19.0	60.0	80.4	64.2	88.0
16	47.6	64.7	43.6	64.0	30.2	20.2	59.3	83.9	64.9	90.2
20	48.0	64.1	44.0	63.8	31.0	20.7	59.3	81.9	66.5	92.9
24	48.1	64.2	44.4	63.7	31.0	21.1	59.6	78.1	67.3	94.2
28	48.1	64.4	44.3	63.6	31.0	21.6	60.1	74.9	67.8	94.5

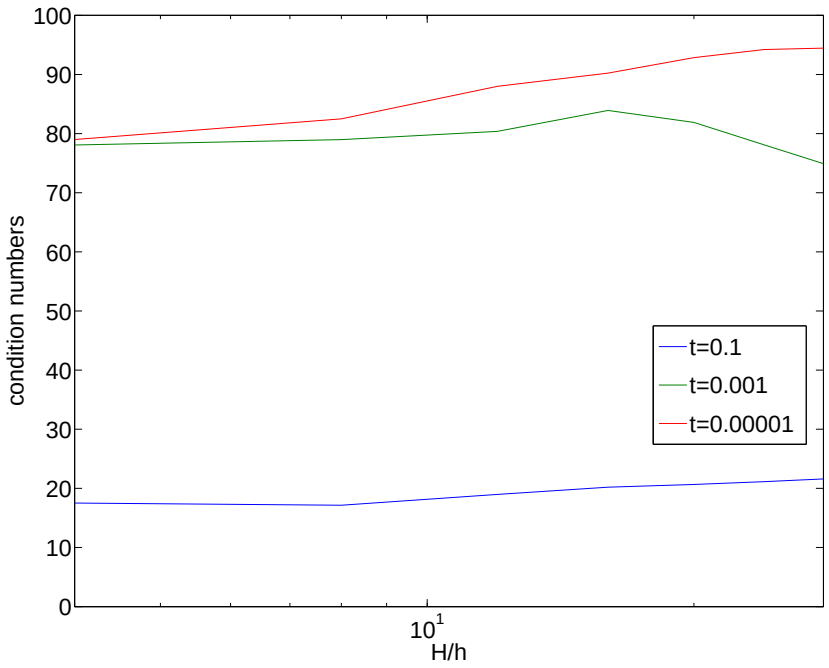

FIG. 8.4. *The condition numbers as a function of $\frac{H}{h}$ with the w quadratic coarse basis functions.*

TABLE 8.6
Results for $h = \frac{1}{72}$, $\frac{H}{h} = 12$, and decreasing $\frac{H}{\delta}$ =12,6,4,3,2.4,2 without the w quadratic coarse basis functions.

$\frac{H}{\delta}$	Iter	cond	Iter	cond	Iter	cond	Iter	cond
t	10		0.1		0.001		0.00001	
12	114.8	1439.2	62.1	96.3	484.9	7153.2	542.0	7387.8
6	93.5	564.2	51.0	56.4	210.4	1070.9	228.9	1324.4
4	73.9	290.6	45.0	47.1	145.3	581.9	162.1	804.3
3	61.4	162.3	40.1	41.1	116.9	438.9	132.6	620.3
2.4	50.9	96.6	36.4	36.7	72.8	216.9	110.1	463.6
2	42.2	59.0	32.7	29.8	83.1	293.0	94.6	398.9

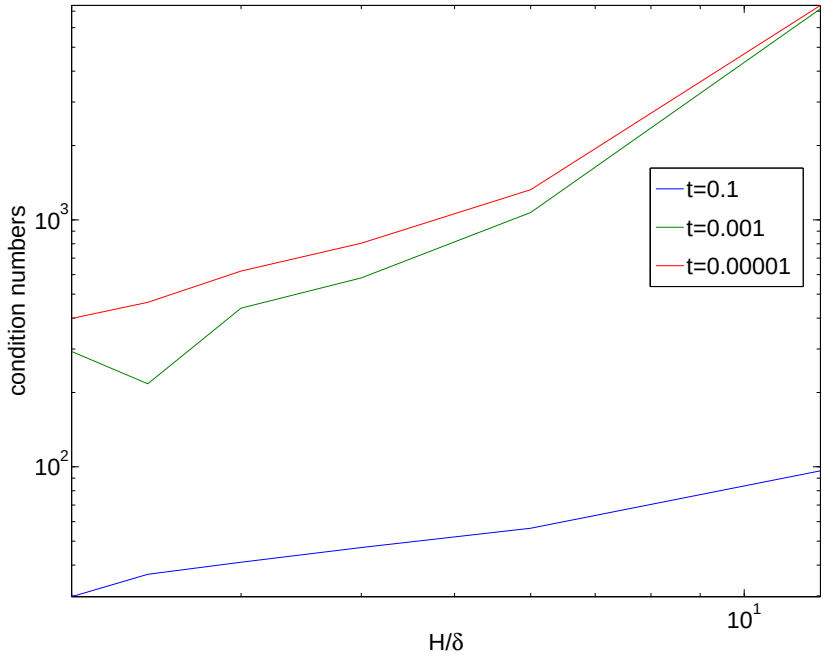

FIG. 8.5. *The condition numbers as a function of $\frac{H}{\delta}$ without the w quadratic coarse basis functions.*

Results with varying $\frac{H}{\delta}$ are given in Tables 8.6 and 8.7 and Figures 8.5 and 8.6. The condition number depends on $\frac{H}{\delta}$. It grows faster with $\frac{H}{\delta}$ when t is small.

TABLE 8.7
Results for $h = \frac{1}{72}$, $\frac{H}{h} = 12$, and decreasing $\frac{H}{\delta}$ =12,6,4,3,2.4,2 with the w quadratic coarse basis functions.

$\frac{H}{\delta}$	Iter	cond	Iter	cond	Iter	cond	Iter	cond
t	10		0.1		0.001		0.00001	
12	116.2	1417.1	61.4	102.3	211.5	960.1	244.4	1033.7
6	94.5	525.2	48.0	47.7	94.7	139.0	102.8	151.8
4	74.9	287.0	41.0	38.4	68.9	77.2	79.0	96.4
3	62.4	165.1	36.0	32.9	60.0	53.9	67.0	67.5
2.4	51.4	96.7	33.0	25.1	53.3	44.0	60.5	57.4
2	42.6	59.2	29.0	22.2	48.2	39.8	55.1	50.9

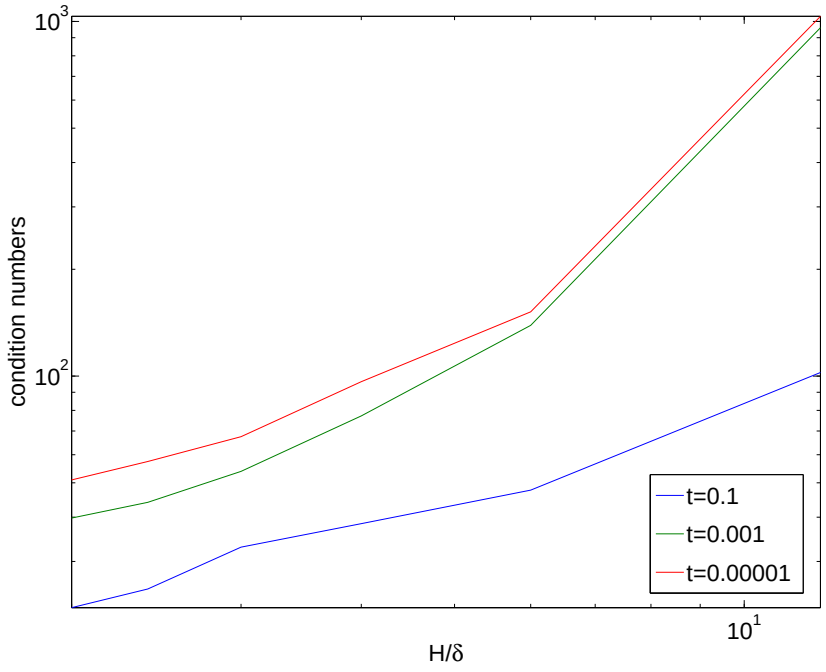

FIG. 8.6. *The condition numbers as a function of $\frac{H}{\delta}$ with the w quadratic coarse basis functions.*

REFERENCES

[1] Douglas N. Arnold, Franco Brezzi, Richard S. Falk, and L. Donatella Marini. Locking-free Reissner-Mindlin elements without reduced integration. *Comput. Methods Appl. Mech. Engrg.*, 196(37-40):3660–3671, 2007.

[2] Douglas N. Arnold and Richard S. Falk. A uniformly accurate finite element method for the Reissner-Mindlin plate. *SIAM J. Numer. Anal.*, 26(6):1276–1290, 1989.

[3] Douglas N. Arnold and Richard S. Falk. The boundary layer for the Reissner-Mindlin plate model. *SIAM J. Math. Anal.*, 21(2):281–312, 1990.

[4] Douglas N. Arnold and Richard S. Falk. Asymptotic analysis of the boundary layer for the Reissner-Mindlin plate model. *SIAM J. Math. Anal.*, 27(2):486–514, 1996.

[5] F. Auricchio and C. Lovadina. Analysis of kinematic linked interpolation methods for Reissner-Mindlin plate problems. *Comput. Methods Appl. Mech. Engrg.*, 190(18-19):2465–2482, 2001.

[6] K.-J. Bathe and F. Brezzi. On the convergence of a four-node plate bending element based on Mindlin-Reissner plate theory and a mixed interpolation. In *The mathematics of finite elements and applications, V (Uxbridge, 1984)*, pages 491–503. Academic Press, London, 1985.

[7] L. Beirão da Veiga. Finite element methods for a modified Reissner-Mindlin free plate model. *SIAM J. Numer. Anal.*, 42(4):1572–1591 (electronic), 2004.

[8] L. Beirão da Veiga, C. Chinosi, C. Lovadina, and L. F. Pavarino. Robust BDDC preconditioners for Reissner-Mindlin plate bending problems and MITC elements. *SIAM J. Numer. Anal.*, 47(6):4214–4238, 2010.

[9] Daniele Boffi, Franco Brezzi, Leszek F. Demkowicz, Ricardo G. Durán, Richard S. Falk, and Michel Fortin. *Mixed finite elements, compatibility conditions, and applications*, volume 1939 of *Lecture Notes in Mathematics*. Springer-Verlag, Berlin, 2008. Lectures given at the C.I.M.E. Summer School held in Cetraro, June 26–July 1, 2006, Edited by Boffi and Lucia Gastaldi.

[10] Dietrich Braess. *Finite elements*. Cambridge University Press, Cambridge, third edition, 2007. Theory, fast solvers, and applications in elasticity theory, Translated from the German by Larry L. Schumaker.

[11] Susanne C. Brenner. A two-level additive Schwarz preconditioner for macro-element approximations of the plate bending problem. *Houston J. Math.*, 21(4):823–844, 1995.

[12] Susanne C. Brenner and L. Ridgway Scott. *The mathematical theory of finite element methods*, volume 15 of *Texts in Applied Mathematics*. Springer, New York, third edition, 2008.

[13] Susanne C. Brenner and Li-yeng Sung. Balancing domain decomposition for nonconforming plate elements. *Numer. Math.*, 83(1):25–52, 1999.

[14] Susanne C. Brenner and Li-Yeng Sung. Multigrid algorithms for C^0 interior penalty methods. *SIAM J. Numer. Anal.*, 44(1):199–223 (electronic), 2006.

[15] Susanne C. Brenner and Kening Wang. Two-level additive Schwarz preconditioners for C^0 interior penalty methods. *Numer. Math.*, 102(2):231–255, 2005.

[16] Franco Brezzi, Klaus-Jürgen Bathe, and Michel Fortin. Mixed-interpolated elements for Reissner-Mindlin plates. *Internat. J. Numer. Methods Engrg.*, 28(8):1787–1801, 1989.

[17] Franco Brezzi, Michel Fortin, and Rolf Stenberg. Error analysis of mixed-interpolated elements for Reissner-Mindlin plates. *Math. Models Methods Appl. Sci.*, 1(2):125–151, 1991.

[18] D. Chapelle and R. Stenberg. An optimal low-order locking-free finite element method for Reissner-Mindlin plates. *Math. Models Methods Appl. Sci.*, 8(3):407–430, 1998.

[19] C. Chinosi, C. Lovadina, and L. D. Marini. Nonconforming locking-free finite elements for Reissner-Mindlin plates. *Comput. Methods Appl. Mech. Engrg.*, 195(25-28):3448–3460, 2006.

[20] Clark R. Dohrmann and Olof B. Widlund. An overlapping Schwarz algorithm for almost incompressible elasticity. *SIAM J. Numer. Anal.*, 47(4):2897–2923, 2009.

[21] Ricardo Durán and Elsa Liberman. On mixed finite element methods for the Reissner-Mindlin plate model. *Math. Comp.*, 58(198):561–573, 1992.

[22] Ricardo G. Durán, Erwin Hernández, Luis Hervella-Nieto, Elsa Liberman, and Rodolfo Rodríguez. Error estimates for low-order isoparametric quadrilateral finite elements for plates. *SIAM J. Numer. Anal.*, 41(5):1751–1772 (electronic), 2003.

[23] Richard S. Falk and Tong Tu. Locking-free finite elements for the Reissner-Mindlin plate. *Math. Comp.*, 69(231):911–928, 2000.

[24] Alexander Iosilevich, Klaus-Jürgen Bathe, and Franco Brezzi. Numerical inf-sup analysis of MITC plate bending elements. In *Plates and shells (Québec, QC, 1996)*, volume 21 of *CRM Proc. Lecture Notes*, pages 225–242. Amer. Math. Soc., Providence, RI, 1999.

[25] Patrick Le Tallec, Jan Mandel, and Marina Vidrascu. A Neumann-Neumann domain decomposition algorithm for solving plate and shell problems. *SIAM J. Numer. Anal.*, 35(2):836–867 (electronic), 1998.

[26] C. Lovadina. A new class of mixed finite element methods for Reissner-Mindlin plates. *SIAM J. Numer. Anal.*, 33(6):2457–2467, 1996.

[27] Mikko Lyly. On the connection between some linear triangular Reissner-Mindlin plate bending elements. *Numer. Math.*, 85(1):77–107, 2000.

[28] Jan Mandel, Radek Tezaur, and Charbel Farhat. A scalable substructuring method by Lagrange multipliers for plate bending problems. *SIAM J. Numer. Anal.*, 36(5):1370–1391 (electronic), 1999.

[29] Dianne P. O'Leary and Olof Widlund. Capacitance matrix methods for the Helmholtz equation on general three-dimensional regions. *Math. Comp.*, 33(147):849–879, 1979.

[30] P. Peisker and D. Braess. Uniform convergence of mixed interpolated elements for Reissner-Mindlin plates. *RAIRO Modél. Math. Anal. Numér.*, 26(5):557–574, 1992.

[31] Barry F. Smith, Petter E. Bjørstad, and William D. Gropp. *Domain decomposition*. Cambridge University Press, Cambridge, 1996. Parallel multilevel methods for elliptic partial differential equations.

[32] Rolf Stenberg. A new finite element formulation for the plate bending problem. In *Asymptotic methods for elastic structures (Lisbon, 1993)*, pages 209–221. de Gruyter, Berlin, 1995.

[33] Andrea Toselli and Olof Widlund. *Domain decomposition methods—algorithms and theory*, volume 34 of *Springer Series in Computational Mathematics*. Springer-Verlag, Berlin, 2005.